



**UNIVERSITA' DEGLI STUDI DI PAVIA**  
Dipartimento di Medicina Molecolare

**Small supernumerary marker chromosomes:  
a legacy of trisomy rescue?**



**Nehir Edibe Kurtas**

Dottorato di Ricerca in  
Genetica, Biologia Molecolare e Cellulare  
XXXI Ciclo – A.A. 2015-2018



**UNIVERSITA' DEGLI STUDI DI PAVIA**

Dipartimento di Medicina Molecolare

**Small supernumerary marker chromosomes:  
a legacy of trisomy rescue?**

**Nehir Edibe Kurtas**

**Supervised by Prof. Orsetta Zuffardi**

Dottorato di Ricerca in  
Genetica, Biologia Molecolare e Cellulare  
XXXI Ciclo – A.A. 2015-2018

## **Abstract**

We studied by a whole cytogenomics approach 12 *de novo*, non-recurrent small supernumerary marker chromosomes (sSMC), detected as mosaics during pre- or postnatal diagnosis. In 11 cases maternal age was increased. Trios genotyping, WGS, and CGH+SNP array, demonstrated that (i) four sSMCs contained pericentromeric portions only, whereas eight had additional non-contiguous portions of the same chromosome, assembled together in a disordered fashion by repair-based mechanisms in a chromothriptic event; (ii) in four cases maternal hetero/isodisomy was detected with a sharp paternal origin of the sSMC in two cases, whereas in a fifth case two maternal alleles in the sSMC region and biparental haplotypes of the homologs were detected. In five other cases the homologs were biparental while the sSMC had the same haplotype of the maternally inherited chromosome. In one case, the sSMC was of paternal origin while the homologs were biparental. These findings strongly suggest that most sSMCs are the result of a multiple-step mechanism, initiated by maternal meiotic non-disjunction followed by post-zygotic anaphase lagging of the supernumerary chromosome and its subsequent insertion within a micronucleus, whose segregation to one of the two daughter cells accounts for the mosaic condition. The sequential micronuclear shattering, re-embedding of the fragmented chromosomal material into the main nucleus where repair occurs, and loss of some fragments, explains both the disordered assembly of most sSMCs and the occurrence of maternal UPD. This mechanism identifies a link between numerical and structural

chromosomal anomalies and underlines that genetic counselling in prenatally detected sSMCs will be problematic.

## **Acknowledgements**

First of all, I would like to thank all the patients and families for their contribution and patience during the project.

Professor Orsetta Zuffardi, I would like to express my special thanks of gratitude for your inestimable supervision since the first day of my PhD. Following your enthusiastic rhythm and always progressive approach on research has been a great school which allowed me to grow as a research scientist.

I would like to thank all our collaborators for their scientific and technical contributions in this project; Massimo Delledonne, Alfredo Brusco, Krystyna Chrzaowska, Albert Schinzel, Daniela Larizza, Silvana Gueneri, Federica Natacci, Maria Clara Bonaglia, Emmanouil Manolakos, Teresa Mattina, Fiorenza Soli, Sabrina Giglio and Thomas Liehr. I would like to specifically thank Professor Massimo Delledonne and his research team in University of Verona for everytime opening their doors to me. Luciano Xumerle, many thanks for your excellent efforts in training me. Lorena Leonerdelli thanks for your initiative hard work in the project.

Debora Vergani, Alessia Russo, Edoardo Errichello, Paolo Reho, Beatrice Casati, Noor Hussain and Camilla Strega, it has been amazing to have such colleagues who turned into friends. Many thanks to each of you for your support and cheerfulness during these three years.

I wish to thank all those helpful - current and former- members of the department of Molecular Medicine; Professor Danesino Cesare, Elena Rossi, Annalisa Vetro, Francesca Novara, Antonella Minelli, Carla Olivieri, Anna Lanfranchi, Marta Diegoli, Silvia Camanini, Marcella Dipli, Antonio Otranto and Sara Plumitallo.

Finally my family, sevgili annem ve babam tükenmeyen desteğiniz ve hayallerinizle başladığım bu yolculuktaki tüm emekleriniz için çok teşekkür ederim, iyi ki varsınız. And Luca Tiezzi, grazie mille per la tua preziosissimo esistenza accanto a me e alla tua famiglia per il loro caloroso supporto durante tutti i miei anni in Italia.

## **Abbreviations**

Alt-NHEJ: alternative non-homologous end joining  
CGH array: array-comparative genomic hybridization  
Chr: chromosome  
CNV: copy number variation  
DSB: double-stranded breaks  
Dup: duplication  
FISH: fluorescent in situ hybridization  
Hom: homologous  
IGV: Integrative Genomics Viewer  
Inv: inversion  
LOH: loss of heterozygosity  
Mat: maternal  
MI: meiosis I  
MII: meiosis II  
MMBIR: microhomology mediated break induced replication  
NA: not available  
NAHR: non-allelic homologous recombination  
NGS: next generation sequencing  
NHEJ: non-homologous end joining  
Pat: paternal  
PCR: polymerase chain reaction  
SNP: single nucleotide polymorphism  
sSMC: small supernumerary marker chromosomes  
STS: Sequence-tagged sites  
UPD: uniparental disomy  
WCP: whole chromosome painting  
WGS: whole genome sequencing

## Contents

Abstract .....	3
Acknowledgements .....	5
Abbreviations .....	6
Contents .....	7
1. Introduction .....	9
1.1 A diagnostic challenge: small supernumerary marker chromosomes..	9
1.2 A new phenomenon: chromothripsis .....	12
2. Aim of the study .....	15
3. Materials and methods .....	16
3.1 Patient Sample.....	16
3.2 Microarray Analysis.....	16
3.3 Fluorescent in situ hybridization (FISH) .....	17
3.4 Genotyping.....	17
3.5 Whole genome Paired-end sequencing (WGS) and data analysis .....	18
3.6 PCR and Sanger Sequencing.....	19
3.7 Accession Numbers.....	19
4. Results .....	21
4.1 sSMC18.....	21
4.2 sSMC2.a .....	23
4.3 sSMC2.b.....	25
4.4 sSMC7.a .....	28
4.5 sSMC17.....	30
4.6 sSMC8.a .....	33
4.7 sSMC11.....	35
4.8 sSMC8.b.....	37
4.9 sSMC1.....	38
4.10 sSMC7.b.....	39
4.11 sSMC8.c .....	40
4.12 sSMC7.c .....	41
4.13 Breakpoint Characteristics and Repeat Elements .....	41

4.14 Disrupted-Fusion Genes .....	43
5. Discussion .....	44
6. Perspectives and future directions.....	55
Supplementary figures and tables .....	56
References .....	83
List of original manuscripts .....	90

## 1. Introduction

### 1.1 A diagnostic challenge: small supernumerary marker chromosomes

A small supernumerary marker chromosome (sSMC) is an extra, structurally abnormal chromosome whose origin cannot be unambiguously identified by conventional banding cytogenetics. In two-thirds of the cases, they are present in mosaic with a normal cell line (Malvestiti et al., 2014). The approximate rate of sSMCs ranges from 0.4/1000 in consecutive newborns to 0.8/1000 in prenatal diagnosis, however their incidence is elevated in subjects with phenotypical/fetal ultrasound abnormalities or reproductive difficulties such as male infertility/multiple abortion (Liehr and Weise, 2007). The estimated rate of *de novo* and familial sSMC is approximately 70% and 30%, respectively (Liehr and Weise, 2007). The incidence of *de novo* sSMCs associates with advanced maternal age as estimated in prenatal diagnoses (Crolla et al., 2005; Malvestiti et al., 2014). In rare cases the sSMC is the product of 3:1 segregation of a parental translocation, such as der(22)t(11; 22)(q23; q11) (Shaikh et al., 1999) but in most cases it is a *de novo* private rearrangement, frequently in a mosaic condition, belonging to that carrier person. According to literature, most of sSMCs are reported to derive from chromosome 15 (44% of all *de novo* sSMCs) (Malvestiti et al., 2014), which are classified into two cytogenetic types of inverted (inv) duplicated (dup) (15) marker chromosomes with different phenotypic consequences (Crolla et al., 1995). One is a small metacentric chromosome, not containing the Angelman syndrome (AS)/Prader-Willi syndrome (PWS) critical region that is mostly associated

with a normal phenotype. The second type is a larger inv dup (15), containing AS/PWS, is associated with an abnormal phenotype. The elevated rate of sSMC15 could be explained by the fact that, markers derived from chr15 could be identified by less-complicated cytogenetic techniques such as DAPI staining. Another examples of recurrent sSMCs other than inv dup (15) are iso(12)p (Schinzel, 1991), iso(18p) (Callen et al., 1990) and inv dup (22) (Mears, 1995) which are large enough to be identified by conventional cytogenetics and have a well-established clinical outcome.

Several mechanisms have been proposed for the formation of inv dup sSMCs. One most likely mechanism is an inter-chromosomal U-type exchange model (Schreck et al., 1977) in which inv dup marker chromosomes could derive from the breakage and consequent fusion of sister chromatids of homolog chromosomes during meiosis. The same mechanism is also used to explain formation of isochromosomes with neocentromere (Voullaire et al., 2001). This hypothesis is then supported by the observation that the frequency of neocentric marker 15 is similar to the rate of inv dup marker 15 (Liehr et al., 2004). However genotype analysis revealed that inv dup marker chromosomes are formed from two copies derived from only a single chromatid end (Murmans et al., 2009). This observation is not well-matched with inter chromosomal U-type exchange model. Thus, an alternative intra-chromosomal exchange model is proposed where U-type exchange may occur between two chromatids of the same chromosome. Additionally, a case study with a neocentric marker derived from Y chromosome produced another conflict on it (Sheth et al., 2009). In summary, U-type exchange model is not compatible for all of the inv dup

marker chromosomes. For the remaining non-recurrent *de novo* SMCs, the exact mechanism for their formation still remains unknown.

Upon detection during prenatal testing a diagnostic challenge arises due to an unambiguous genotype-phenotype correlation. According to empirical data from diagnostic surveys, the risk of manifesting clinical abnormalities in *de novo* sSMC carriers ranges between 18% and 26% (Graf et al., 2006). Several factors such as genetic content and size of sSMC, degree of mosaicism and involvement of uniparental disomy (UPD) might alter the risk associated with abnormal phenotypes. The incidence of UPD cases in combination with sSMC is rare (Kotzot, 2002; Liehr et al., 2015). According to the literature, most of cases showed a maternal UPD with *de novo* and mosaic state of sSMC. Further complexity to the genetic counselling is given by the finding that some sSMCs are constituted by non-contiguous regions of the same chromosome (Vetro et al., 2012). According to all these points, namely maternal age effect, presence of mosaicism, association with UPD, and noncontiguity of the chromosomal regions constituting the sSMC, we assume that constitutional sSMC were the final result of maternal chromosome non-disjunction leading to a trisomic zygote that in the early embryogenesis undergo to events of total and partial trisomy rescue in different cells, thus resulting in a mosaic embryo with a normal cell line (complete trisomy rescue) and a second one with the sSMC (partial trisomy rescue). A mosaicism with a normal and a trisomic cell line is reported in 2-3% of chorion villi (Kalousek and Dill, 1983) and it is assumed that the rescue of an entire supernumerary chromosome occurs via anaphase lagging. This theory was supported by a recent study which showed, using live-cell imaging, a significant increase in the rate of

anaphase lagging in trisomic cell lines (Nicholson et al., 2015). Anaphase lagging may result in the formation of a micronucleus where misaligned chromosome(s) is isolated. Recently, It was demonstrated that DNA trapped in micronuclei may undergo catastrophic breakages where random reassembly of the fragmented pieces resulted in several rearrangements within the isolated DNA (Zhang et al., 2015). This phenomenon is termed chromothripsis (Stephens et al., 2011).

#### 1.2 A new phenomenon: chromothripsis

Chromothripsis has been characterized by the localized shattering of one or more chromosomes followed by the random reassembly of the resulting chromosomal pieces, with the loss of others (Stephens et al. 2011). It was first discovered in a patient with chronic lymphocytic leukemia, where 42 chromosomal rearrangements localized at the q arm of single chromosome 4. Soon after its discovery in cancer genomes, chromothripsis has been shown to occur also in patients with congenital disorders (W. P. Kloosterman et al. 2011; Chiang et al. 2012; Bertelsen et al. 2015; Wigard P. Kloosterman et al. 2012).

Several mechanisms have been introduced to explain the complex rearrangements of chromothripsis. One early idea was chromothripsis might be triggered by ionizing radiations causing DNA damage, generating double-stranded breaks (DSB) which might have undergone aberrant repair (Stephens et al., 2011). Given that both DSB repair mechanisms, non-allelic homologous recombination (NAHR) (for recurrent copy number variations) and non-homologous end joining (NHEJ), can be the major cause of many of chromosomal rearrangements (Lupski and Stankiewicz, 2005), genotoxic

induced DSBs would have been a plausible idea. However, it was still not sufficient to explain how genotoxic agents damage only one chromosome while the other chromosomes remained undamaged. According to recent studies regarding breakpoint cloning in patients with congenital defects, both NHEJ (Kloosterman et al., 2011) and/or microhomology mediated end joining (MMEJ) appear to be associated with the repair of the numerous breakages in chromothripsis chromosomes, and excluded other mechanisms such as NAHR (Malhotra et al., 2013). On the other hand, alternate mechanisms based on DNA replication errors, such as fork stalling and template switching (FoSTeS) (Lee et al., 2007) and microhomology-mediated break-induced replication (MMBIR) (Hastings et al., 2009), have been proposed. However replication error based mechanisms might explain chromoanasythesis, another sharply localized form of complex chromosomal rearrangement, characterized by the large series of non-recurrent copy number gains and losses on a single chromosome (Liu et al., 2011). Recently, single cell sequencing experiments provided direct evidence that micronuclei can generate chromothripsis both in cancer and developmental disorders. According to this model, mitotic errors might produce lagging chromosome(s) which is isolated into a physical nuclear structures called micronuclei (Crasta et al., 2012). Isolated chromosome might undergo extensive DNA damage with all hallmark rearrangements of chromothripsis due to asynchronous DNA replication in respect to the main nucleus. Several defects of micronuclei were described in order to explain catalytic origin of chromothripsis. These are (i) defective replication and repair mechanism (Terradas et al., 2009; Crasta et al., 2012; Hatch 2013) (ii) increased fragility of micronucleus (Hatch, 2013), (iii) decreased nuclear

pores and limited transport capability (Crasta et al., 2012; Hatch, 2013; Hoffelder et al., 2004), (iv) asynchrony in DNA replication between micro- and main nucleus leading to premature condensation and breakage of the chromosome contained in the micronucleus (Sen et al., 1989; Obe et al., 1975). Even though mechanistic questions for micronuclei still remains unclear, pulverization of chromosome in micronuclei is a well-demonstrated mechanism in order to explain how chromothripsis might occur restrictedly on a single or few chromosomes.

## 2. Aim of the study

In this study, we hypothesize that most *de novo* constitutional non-recurrent small supernumerary marker chromosomes (sSMC) are the remnant of a supernumerary chromosome present in trisomic embryos, which undergoes a chromothripsis event resulting in its massive fragmentation with loss of some portions and disordered reunion of the remaining ones. To investigate this, we collected DNA from 12 cases detected with non-recurrent *de novo* sSMCs, and from their parents, all in mosaic with a normal cell line. We combined traditional cytogenetics with comprehensive cytogenomic approach in order to reveal;

- (i) parental origin of the sSMC and its corresponding homologous chromosomes to investigate its possible trisomic origin
- (ii) genomic construction and breakpoint analysis of sSMC to find any signature of a chromothripsis event.

### **3. Materials and methods**

#### **3.1 Patient Sample**

We established a collaboration study to collect cases with small supernumerary marker chromosomes (sSMC) as detected by previously performed conventional cytogenetics and microarray analysis (Supp. Table S1). The DNA samples were requested from both patients and their parents. Informed consents were obtained for the genetic analysis from the parents in the original host institutes.

#### **3.2 Microarray Analysis**

Microarray analysis with Agilent SurePrint G3 combined comparative genomic hybridization and small nuclear polymorphism array (CGH+SNP array) 4x180K (G4890A) was performed in the following cases; sSMC1 (trio), sSMC2.a (trio), sSMC2.b (trio), sSMC7.a (patient only), sSMC7.b (trio), sSMC7.c (trio), sSMC8.a (trio), sSMC8.b (trio), sSMC8.c (trio), sSMC11(prenatal, trio) and sSMC17 (trio). SurePrint G3 Human G3 CGH 1x1M (G4447a) was performed in the case sSMC7.c. All nucleotide positions refer to the Human Genome, Feb 2009 Assembly (GRCh37, hg19). Data analysis regarding copy-number changes and copy-neutral variations, including loss of heterozygosity (LOH) and uniparental disomy (UPD) was performed by CytoGenomics software v5.0 (Agilent Technologies).

### 3.3 Fluorescent in situ hybridization (FISH)

FISH analysis was performed on metaphase spreads by standard procedure. For case sSMC2.b, metaphase spreads were analyzed by chromosome 2 specific centromeric probe (D2Z1, red, Cytocell), SATB2(2q33.1, red, Agilent) and PAX3(2q36.1, green, Agilent). For case sSMC7.a, fluorescently labelled BAC probes RP11-144H20 (red), RP11-340I6 (purple) and RP11-3N2 (yellow) were used. For case sSMC1, metaphase spreads were analyzed by chromosome 1 specific centromeric probe (D1Z7, red, Cytocell) and whole chromosome paint probe (WCP1, green, Cytocell). For cases sSMC7.b and sSMC7.c metaphase spreads were analyzed by chromosome 7 specific centromeric probe (D7Z1, red, Cytocell). For case sSMC8.a, metaphase spreads were analyzed by chromosome 8 specific centromeric probe (D8Z2, green, Cytocell). For case sSMC11, metaphase spreads were analyzed by chromosome 11 specific centromeric probe (D11Z1, red, Cytocell). For the cases with sufficient material, further FISH analysis was performed with telomere-specific pan-telomeric peptide nucleic acid (PNA) probe (PNA FISH kit/Cy3, Dako, Denmark), which recognizes the consensus sequence (TTAGGG)<sub>n</sub> of human pan-telomeres. Absence of the signal is interpreted as a ring chromosome.

### 3.4 Genotyping

Genotyping was performed in family trios in 9 cases: sSMC1, sSMC2.a, sSMC2.b, sSMC7.b, sSMC8.a, sSMC8.b, sSMC8.c, sSMC11 and sSMC17. In case sSMC7.a, we lacked maternal DNA to complete the analysis. PCR amplification of microsatellites located within duplicated and normal copy regions were performed with fluorescently labelled primers (5-Fam and

Hex) (Sigma Aldrich, Darmstadt, Germany). PCR products were analysed on an ABI PRISM® 310 Genetic Analyzer and the sizes of different alleles were examined using Peak Scanner™ software v2.0.

### **3.5 Whole genome Paired-end sequencing (WGS) and data analysis**

Paired-end libraries were generated from 2,5 µg DNA isolated from peripheral blood leukocytes of postnatal subjects. For the case sSMC2.b, DNA was obtained from abortive tissue (sternum). For the cases sSMC11, DNA was extracted from amniotic fluid. The sequencing library is prepared using Illumina's TruSeq DNA PCR Free kit (San Diego, CA, USA) by random fragmentation of the DNA sample with Covaris system, followed by 5' and 3' adapter ligation. Libraries were sequenced using the Illumina HiSeq X Ten with 150PE reads. Reads from the fastq files were mapped to the human reference genome GRCh37/hg19 using Isaac Genome Alignment Software (version iSAAC-03.16.06.06) (Raczy et al., 2013). In order to identify large duplications, constituted sSMC structure, coverage graphs were created by an in house script that uses samtools (with "depth" option) to calculate the average coverage on not overlapping 1000bp windows over the whole chromosome length and gnuplot program to produce the figures. Structural variants were called by Lumpy (version 0.2.12) (Layer et al., 2014) and Manta (version: 0.29.6) (Chen et al., 2016), which were used to identify exact breakpoints of duplicated regions and further rearrangements assumed to be involved in sSMC. The breakpoints at the duplicated sites were manually checked in Integrative Genomics Viewer (IGV) genome browser (Version 2.3.72) (Robinson et al., 2011) and the marker chromosomes were reconstructed according to the orientations of discordant

reads detected on each breakpoint. The predicted fusion junctions were verified by Sanger sequencing.

### 3.6 PCR and Sanger Sequencing

The DNA sequence of breakpoint junctions are constructed according to the human reference genome (GRCh37/hg19) using the UCSC Human Genome Browser. Primers for breakpoints of predicted structural variations were designed using primer3 software. Sufficient PCR products for each breakpoint junction were yielded using GoTaq® G2 Flexi DNA polymerase (Promega) with an elongation times of 1 min for 40 cycles. Sanger sequencing reads were examined with Chromas software.

### 3.7 Accession Numbers

Reconstruction of sSMC and clinical data have been archived in publically available database for sSMC (<http://ssmc-tl.com/sSMC.html>). The accession numbers for the cases sSMC1, sSMC2.a, sSMC2.b, sSMC7.a, sSMC7.b, sSMC7.c, sSMC8.a, sSMC8.b, sSMC8.c and sSMC11 reported in this paper are: 01-Uu-3, 02-Ud-1, 02-Ud-2, 12L0080, 07-Uu-10, 07-Uu-9, 2010B110, 08-W-p23.1/2-1, 08-Ud-6 and 11-Ud-2.

**PCR Primers used in breakpoint validation**

Name	Sequence (5->3)	PCR Product Size (bp)	Annealing Temp (°C)
sSMC18_18b-18d_F	TTGGTCTGCCTTCTTCCAC	795	61
sSMC18_18b-18d_R	TGATGAGATTGCTTGCTTCTT		
sSMC18_RingJ_F	CCCTAATGCAGTGAGTGGCT	683	63
sSMC18_RingJ_R	CGAAATCCCCAAAGCTAGCC		
sSMC2.a_2c-2f_F	GGGCTAAGAATGCAAATGGA	830	62
sSMC2.a_2c-2f_R	CCAACCTCCCTGCTCTACACC		

3. Materials and methods

sSMC2.b_2b-2d_F	CCCTGAGGCTGGATAGAACA	831	62
sSMC2.b_2b-2d_F	CCCATCCCAGAGTCTGTGTT		
sSMC7.a_7d-7b_F	AGTGCTTTGAGGCCTATGGT	788	62
sSMC7.a_7d-7b_R	GAGCCCAGCAATTTGAGGTC		
sSMC7.a_7e-7d_F	TGGGAAATGAAGGGATGGGC	505	65
sSMC7.a_7e-7d_R	TTTGCTCTCACATTGGGACA		
sSMC17_17d-17b_F	TGTTGGATATGGGGTTTGCA	457	63
sSMC17_17d-17b_R	CCGAGGTGACATCTGCCTAT		
sSMC8.a_RingJ_F	TCTGAAATGGCCTGCTATC	813	62
sSMC8.a_RingJ_R	CAGATTTGAGCTGGGAGGAG		
sSMC8.b_RingJ_F	ATTGAAAGTGGGCTGTGCTG	855	63
sSMC8.b_RingJ_R	GAGCCCTCCACTCTTCATT		
sSMC11_g-a_F	TCCTCTCCAACCAACTCC	819	62
sSMC11_g-a_R	CACTCCCTCCTTGAACCACT		
sSMC11_f-g_F	TCCTCTGTCCCTCCACTAA	800	62
sSMC11_f-g_R	ATCCCTGGGTTTGAGTCCTG		
sSMC11_k-l2_F	CCAGAGGAGAGAAGCTGAGG	796	62
sSMC11_k-l2_R	CCCGCCTGTGTTTTCTTAG		
sSMC11_d-e_F1	GTGGGCTACTGGATGGAGAG	785	62
sSMC11_d-e_R1	CAGACTCCCACTGCTGTTC		
sSMC11_a-b_F	CATGATGGCTGGTTTCCGG	850	65
sSMC11_a-b_R	CCACCACTTCTGACCACA		
sSMC11_b-d_F	AGGTAGGCGAGGTCTTTCAA	801	61
sSMC11_b-d_R	CCATGACCACCTCCTCTGTT		
sSMC11_l-H1_F	AAACAAATACACCGTGGGCC	788	65
sSMC11_l-h1_R	TTCCCATATTCCACCCAG		
sSMC11_c-j_F	TGCTTGCAGTCTCCTTACCT	777	61
sSMC11_c-j_R	TGGCATTGTTACTGACCAGC		

## 4. Results

### 4.1 sSMC18

This was a previously studied case where a sSMC was detected in a female patient born with a psychomotor retardation involving a pattern of dysmorphic features (Rothlisberger et al., 2000). She was the second child of healthy and unrelated parents. Cytogenetic analysis showed a mosaic sSMC present in 70% of metaphases obtained from blood lymphocyte cultures, while father and mother had normal karyotypes. Combined microdissection and reverse painting experiments on metaphase chromosomes revealed that the sSMC was formed by two non-contiguous regions of chromosome 18, 18p11.1->18q11.1 and 18q12.3->18q21.1. Microsatellite analysis performed on the trio, with primers targeted to duplicated regions, showed double peaks with a maternal origin of the intenser band, whereas the microsatellites lying outside of the marker region suggested a biparental inheritance of the normal homologous chromosomes 18.

Consistent with the preliminary cytogenetics data, coverage plot of chromosome 18 from WGS revealed two non-contiguous duplications (Figure 1A). The precise breakpoints of the two duplications were determined; fragment 18b (chr18:18520343-18594804) and fragment 18d (chr18:41472065-49040431) (Supp. Table S3). The mean coverage of duplicated portions were calculated as 56.4x and 55.18x for the fragment 18b and 18d, respectively, while the normal copy region has the mean coverage of 38.0x. The orientation of discordant reads detected at the

breakpoints of duplications were used in order to reconstruct the sSMC18, which was then confirmed by PCR and Sanger sequencing. Discordant reads at the left side of fragment 18d (chr18:41472065) mapped to the reads detected at the left side of the fragment 18b (chr18:18594804). Discordant reads at the right side of the fragment 18d (chr18:49040431) contained 86bp sequence having 96% nucleotide match with human alphoid repetitive DNA L1.84 of chromosome 18, supporting a ring closure junction (Supp. Figure S1A). As a result, sSMC18 was constituted by the fusion of the two duplicated segments in the same order of reference genome, producing two fusion junctions named as BPJ\_18b(+)\_18d(+) (chr18:18594804::chr18:41472065) and ring closure junction RingJ\_18d(+)\_Alphoid (chr18:49040431::Alphoid) (Figure 1B). Following Sanger sequencing demonstrated the fusion junction between fragment 18d and alphoid DNA L1.84, having microhomology of 4 bases (GAGC) at the junction (Supp. Figure S1B). Breakpoint signature at the fusion junction BPJ\_18b(+)\_18d(+) involved a microhomology of 4 bases (ATGG) (Supp. Figure S1B). Absence of telomere sequences, as demonstrated by metaphase FISH analysis using telomere specific (TTAGGG) PNA probes, supported its ring constitution (Figure 1C).

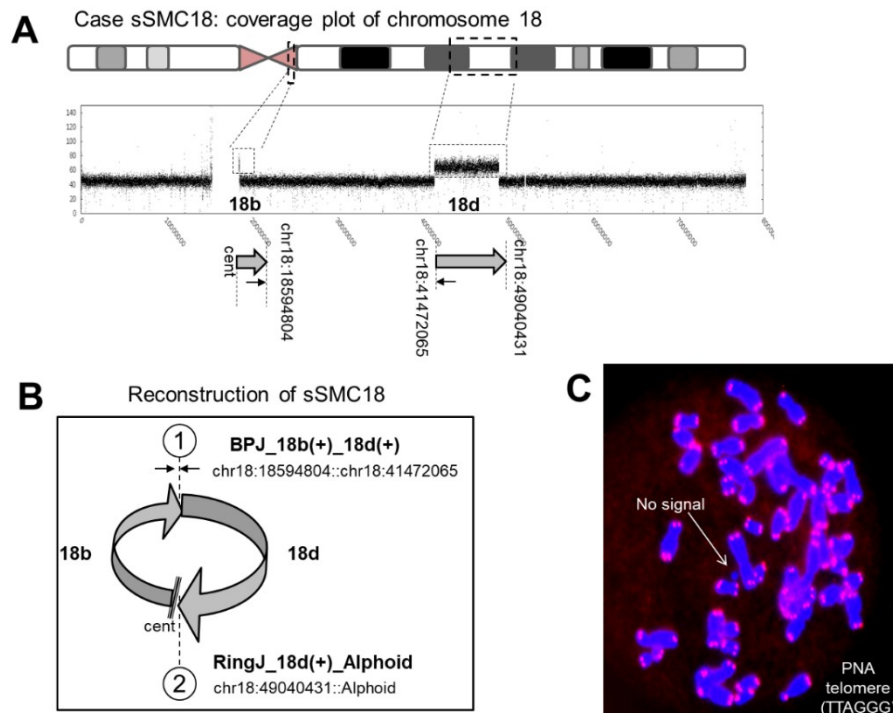


Figure 1: (A) NGS coverage plot analysis of chromosome 18 indicated the two duplicated portions, illustrated by block arrows (grey), 18b (chr18:18520343-18594804) and 18d (chr18:41472064-49040431). Discordant reads (illustrated by the two thin black arrows) at the start side of fragment 18d (chr18:41472065) mapped to the reads detected at the end side of the fragment 18b (chr18:18594804). (B) Schematic representation of sSMC18 with the fusion junctions BPJ\_18b(+)\_18d(+) (number 1) and RingJ\_18d(+)\_Alphoid (number 2) (fragments not in scale). (C) FISH analysis by telomere-specific PNA telomeric probe demonstrated the absence of telomeric sequence on the marker chromosome (indicated by an arrow). For further details, see supplemental data (Supp. Figure S1).

#### 4.2 sSMC2.a

Peripheral blood karyotype analysis in a patient with global developmental delay revealed a mosaicism regarding a cell line with normal karyotype, a cell line with a marker chromosome and a cell line with multiple markers: 47,XX,+mar(51%)/48,XX,+2mar(37%)/46,XX,(12%).

Following CGH+SNP array (4x180K) analysis in trio showed a *de novo* mosaic amplification of a region spanning from 2p11.2 to 2q12.1 (chr2:89143658-102866253) and a *de novo* duplication of the 2q12.2 (chr2:106604839-107241592) in the patient (Supp. Figure S2A). CGH+SNP array in trio suggested a biparental origin of homolog chromosome 2 with maternal origin of marker. Microsatellite analysis in trio targeting duplicated region revealed a maternal origin of marker with an intenser band of maternal allele (Supp. Table S2). Duplications spanning from 2q11.1 to 2q12.2 were delineated by the coverage plot analysis of WGS data. We identified four separate duplicated regions named as 2b, 2c, 2d and 2f (Supp. Table S3). Because the duplicated fragments, mainly fragments 2b and 2c were located at poorly covered regions, NGS analysis was limited to capture the exact breakpoints for these fragments (Supp. Figure S2B-G). We defined the breakpoints of these fragments according to their different level of copy number gain. As a result, four duplicated regions, 2b (chr2:95326241-98026880) with the mean coverage of 75.56x, 2c (chr2:98058590-102613162) with the mean coverage of 59.04x, 2d (chr2:102613162-102867861) with the mean coverage of 51.43x and 2f (chr2:106555286-107260062) with the mean coverage of 49.6x were defined (Figure 2A). The mean coverage of normal copy region of chromosome 2 was calculated as 38.2x. Therefore fragment 2b has a relative coverage of 3~4x, fragment 2c has 3x, while fragment 2d and 2f have of 2~3x. We could detect discordant reads only at the end of the fragment 2c, indicating a novel fusion junction between fragment 2c and fragment 2f (chr2:102613162::chr2:106555286) (Figure 2B). The Sanger validation of the junction revealed a microduplication of 2 bp (TA) at the junction point

(Supp. Figure S2H). Because the sample was no more available, we did not perform confirmatory FISH analysis.

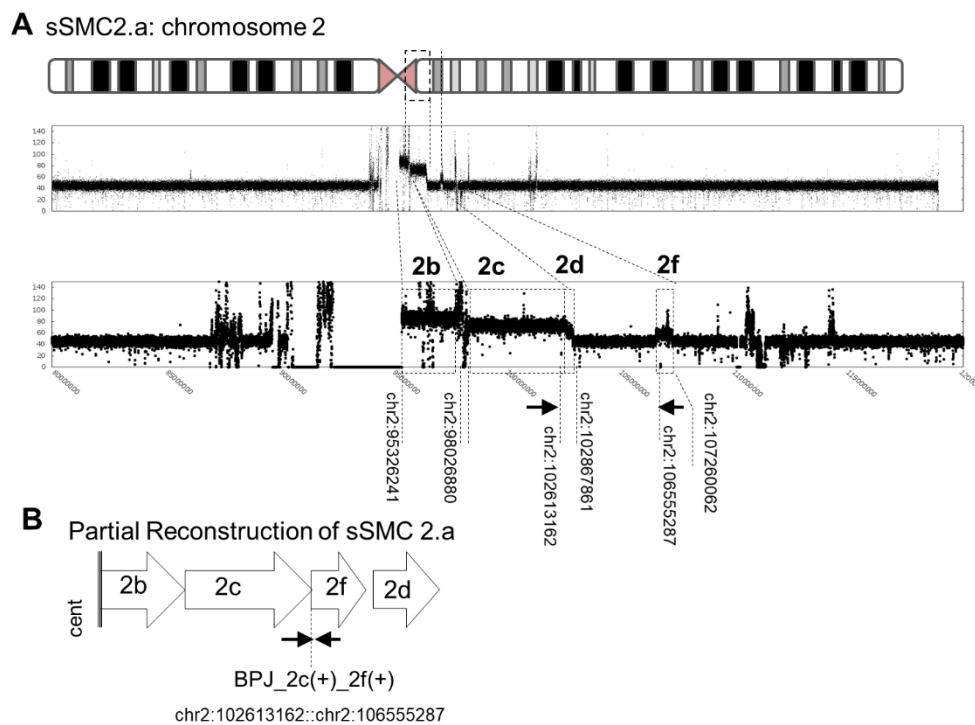


Figure 2: (A) NGS coverage plot analysis of chromosome 2 shows four duplicated regions, 2b (chr2:95326241-98026880), 2c (chr2:98058590-102613162), 2d (chr2:102613162-102867861), and 2f (chr2:106555286-107260062). (B) Schematic illustration of Ssmc2.A. Discordant reads (black thin arrows) indicated a novel fusion junction between fragment 2c and fragment 2f (chr2:102613162::chr2:106555286) (fragments not in scale). For further details, see supplemental data (Supp. Figure S2).

### 4.3 sSMC2.b

Cytogenetic analysis on the chorionic villi from a fetus showing multiple ultrasound abnormalities detected a supernumerary marker chromosome. CGH+SNP array (4x180K) on the trio revealed *de novo* copy-number gains of two non-contiguous regions of chromosome 2 in fetal DNA (Supp.

Figure S3A). The two copy-number gains involved the chromosomal segments spanning from 2q11.1 to 2q11.2 (chr2:95561604-97547601) and from 2q32.2 to 2q36.3 (chr2:191,482,943-230,254,104). Informative SNPs at the LOH copy-neutral regions located outside of sSMC2.b, 2p24.3p14, 2q11.2q12.3, 2q14.1q14.3 and 2q36.3q37.3, indicated a maternal uniparental disomy (UPD). FISH analysis with probes targeting D2Z1, SATB2 (2q33.1) and PAX3 (2q36.1) confirmed the array interpretation (Supp. Figure S3B-D). Microsatellite analysis with the probes targeting duplicated and copy-neutral regions demonstrated maternal heterodisomy for chromosome 2 with a paternal origin of marker chromosome 2 (Supp. Table S2). Using WGS, the precise breakpoints of two non-contiguous duplications sSMC2.b\_2b (chr2:95326171-97556545) and sSMC2.b\_2d (chr2:191545235-230273236) were determined (Figure 3A, Supp. Table S3). The mean coverage of 63.06x and 62.04x were calculated for the fragments 2b and 2d, respectively. The mean coverage of the diploid portion of chr2 was 42.9x. The orientation of paired-reads at the breakpoints suggested a disordered assembly of the segments where the fragment 2d was inverted and fused with fragment 2b producing a novel fusion junction BPJ\_2b(+)\_2d(-) (chr2:97556545::chr2:230273236). The breakpoint characterization of the junction by Sanger sequencing revealed a blunt fusion of the segments without a microhomology (Supp. Figure S3E). The absence of telomeric sequences, as shown by FISH with telomere probes, suggested a ring shape of the marker chromosome (Figure 3B). We did not detect further discordant reads to confirm a potential fusion at the centromeric region. Instead at the start site of the duplicated fragment 2d, we detected discordant reads chr2:191545235, mapping to chromosome 9,

chr9:67216590, suggesting a fusion between two genomic regions. Despite the lack of Sanger validation due to the AluY and L1ME4b repeats at the breakage site of chromosome 9, this finding might indicate involvement of other genomic regions at the fusion junction of a ring shaped sSMC2.b (Supp. Figure S3F).

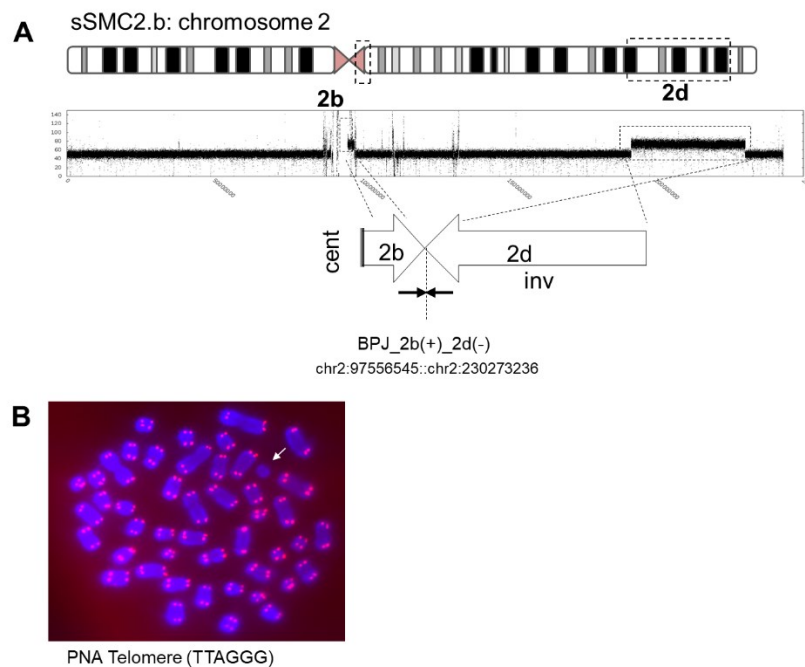


Figure 3: (A) Coverage plot analysis of chromosome 2 from NGS data is shown. Using WGS, the precise breakpoints of the two non-contiguous duplications, fragment 2b (chr2:95326171-97556545) and 2d (chr2:191545235-230273236), were defined. The orientation of paired-reads at the breakpoints suggested a disordered assembly of the segments where the fragment 2d was inverted (inv) and fused with fragment 2b producing a novel fusion junction BPJ\_2b(+)\_2d(-) (chr2:97556545::chr2:230273236). (B) FISH analysis by using telomere specific (TTAGGG) PNA probes showed the absence of telomere sequence in sSMC2.b. For further details, see supplemental data (Supp. Figure S3).

#### 4.4 sSMC7.a

The patient was a female child presenting with the signs of Silver Russell syndrome: pre- and postnatal growth-retardation, small and triangular face. At the age of 4.5 years, both her stature and weight were  $\ll$  3rd percentile. Cytogenetic analysis of blood lymphocyte cultures showed a sSMC in 53% of the metaphases. Using FISH, the sSMC was positive for probe RP11-10F11, indicating its chromosome 7 origin. CGH+SNP array on the proband revealed copy number gain of a single region from 7q11.1 (chr7:61274531) to 7q11.21 (chr7:63664030) (Supp. Figure S4A). LOH was detected in whole chromosome 7 with 98% of SNPs on chromosome 7 having homologous alleles, which indicates a uniparental disomy. Microsatellite analysis performed on the trio revealed a maternal hetero/iso disomy UPD7 (Supp. Table S2).

As obtained by WGS data, the coverage plot of whole chromosome 7 and the discordant reads at the sides of change in coverage facilitated to reconstruct the marker chromosome 7. We detected three separate fragments named as sSMC7.a\_7b (chr7:57,645,143-62,050,000), sSMC7.a\_7d (chr7:62394403-63674966) and sSMC7.a\_7e (Chr7:63674967-63681708) (Figure 4A, Supp. Table S3). Although an uneven coverage of chromosome 7 challenged the determination of mean coverage of entire portion of each duplicated fragments, mean coverage at the good coverage sides of fragments 7b, 7d and 7e were calculated as 47.43x, 55.58x and 43.78, respectively, while the diploid region was 34.46x. Thus, the mean coverage of fragment 7e was relatively lower than the other fragments. FISH analysis with BAC probes, RP11-144H20 (Chr7:61968709-62155949) targeting fragment 7b, RP11-340I6 (chr7:63271383-63465453) and RP11-3N2

(chr7:63427818-63579385) targeting fragment 7d, confirmed the chromosomal content of sSMC7.a (Supp. Figure S4B). Discordant reads detected at the breakpoints of the duplicated portions revealed two novel fusion junctions, BPJ\_7e(+)\_7d(-) and BPJ\_7d(-)\_7b(+), where fragment 7d was inverted and embedded in between fragments 7e and 7b (Figure 4B). The sequence characterization of fusion junctions by Sanger sequencing showed a 17bp insertion at the fusion junction at BPJ\_7e(+)\_7d(-) (Supp. Figure S4C). BLAT analysis (<https://genome.ucsc.edu>) of insertion showed a 100% nucleotide match with LINE-1 (L1ME4a) element mapped on chromosome 9. The junction between inverted fragment 7d and 7b, BPJ\_7d(-)\_7b(+) showed a blunt fusion (Supp. Figure S4C). Loss of telomeric sequence is demonstrated by the absence of PNA telomere probe on sSMC7.a (Figure 4C).

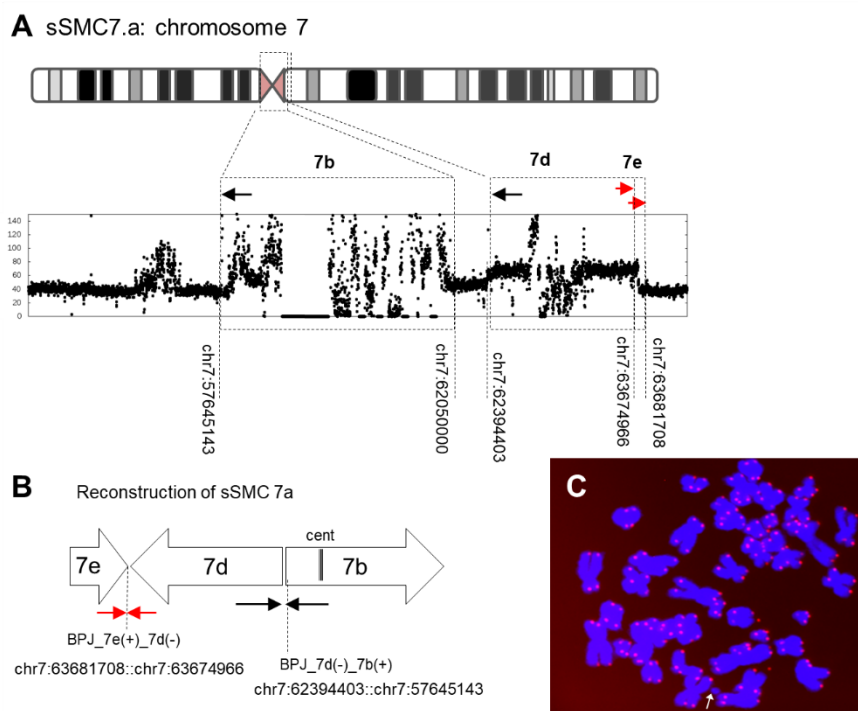


Figure 4: (A) As obtained by WGS data, we defined three separate fragments named as 7b (approximately: chr7:57,645,143-62,050,000), 7d (chr7:62394403-63674966) and 7e (Chr7:63674967-63681708). (B) Discordant reads detected at the breakpoints of the duplicated portions revealed two novel fusion junctions, BPJ\_7e(+)\_7d(-) and BPJ\_7d(-)\_7b(+), where fragment 7d was inverted and embedded in between fragments 7e and 7b. (C) FISH analysis by telomere specific (TTAGGG) PNA probes showed the absence of telomere sequence. For further details, see supplemental data (Supp. Figure S4).

#### 4.5 sSMC17

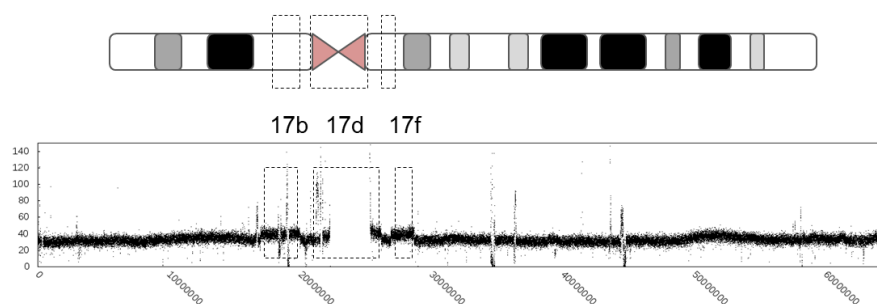
This was a previously studied case where a sSMC17 was detected in a male patient presenting with a mild dysmorphic features and severe developmental delay (Vetro et al. 2012). He was the second child of healthy and nonconsanguineous parents. Cytogenetic analysis on blood lymphocyte cultures showed a mosaic sSMC in 80% examined cells. Using FISH, the sSMC was positive for the probes CEP17 (chromosome 17 centromere) and

RP11-403E9 (17q11.2) whereas the probe RP11-746M1 (17p11.2) did not map on the sSMC. Following array-CGH analysis demonstrated the three non-contiguous duplications, 2.9Mb (17p11.2), 319kb (17q11.1), and 1.8Mb (17q11.2), constituting the sSMC17. Genotype of a microsatellite locus (D17S2196) located on the duplicated site of chromosome 17 suggested a maternal origin of sSMC 17 with two alleles coming from mother. UPD of chromosome 17 was excluded by SNP data and microsatellite genotyping (Supp. Table S2).

Duplicated fragments, named as 17b, 17d and 17f, were predicted based on the increase in the coverage at the plot (Figure 5A). Because the duplicated regions, mainly the start site of centromeric duplication (fragment 17d), were located at copy number varied regions, the detection of its approximate breakpoint was challenged. While for the remaining breakpoints, the relatively sharp increase in the coverage and the detection of the discordant reads at the breakpoints allowed us to detect their exact or approximate breakpoints. As a result, three duplicated fragments are defined as sSMC17\_17b (chr17:16,958,801-19,954,445), sSMC17\_17d (chr17:21,700,105-26,140,775) and sSMC17\_17f (chr17:26,893,603-28,644,236) (Supp. Table S3). Mean coverage of each fragments 17b, 17d and 17e were calculated as 33.25x, 34.5x and 32.8x, while the mean coverage of normal-copy region was 29.2x. The slight increase in the coverage confining the duplicated region is probably due to poor sample quality. Discordant reads at the breakpoints revealed a disordered reassembly of two fragments, producing a novel fusion junction between fragments 17d and 17b, BPJ\_17d(+)\_17b(+) (chr17:21700105-26140775::chr17:16958801-19954445). Sanger sequencing confirmation of

this fusion junction revealed a 36bp insertion (Supp. Figure S5A). BLAT analysis (<https://genome.ucsc.edu>) of insertion showed a 96% sequence match with LINE 1 (L1MB8) element. We identified further discordant reads at the end site of the third duplicate, fragment 17f, suggesting a fusion junction between chr17:28644215 and centromeric region chr17:22251490 (Figure 5B, Supp. Figure S5B). However repeat elements at the centromeric site impeded the breakpoint cloning.

### A sSMC17: chromosome 17



### B Reconstruction of sSMC17

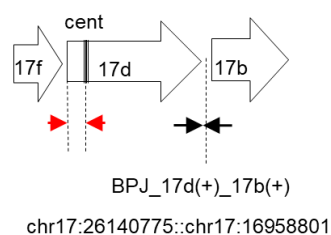


Figure 5: (A) Coverage plot analysis of whole chromosome 17 from NGS data is shown. Three duplicated fragments are defined as 17b (chr17:16,958,801-19,954,445), 17d (chr17:21,700,105-26,140,775) and 17f (chr17:26,893,603-28,644,236). (B) Schematic illustration of the reconstruction of sSMC17. Discordant reads detected at the breakpoint junctions and illustrated as arrows (black), revealed a disordered reassembly of two fragments, producing a novel fusion junction between 17d and 17b, BPJ\_17d(+)\_17b(+) (chr17:26140775::chr17:16958801). Discordant reads (red) at the end site of the third duplicate, fragment 17f, suggesting a fusion junction between chr17:28644215 and centromeric region (cent). For further details, see supplemental data (Supp. Figure S5).

#### 4.6 sSMC8.a

The patient was a male child presenting with the signs of Pierre Robin sequence. Initial karyotype analysis on PBL cells suggested presence of multiple sSMCs including ring chromosome 4, r(4)::p12→q12::), ring chromosome 8 r(8)::p11.21→q11.21::) and ring chromosome 11 r(11)::p11.12→q11.1::). CGH+SNP array analysis in trio showed a de novo duplication of a pericentric region, hg19:8p11.21p11.1 (40089168-53487330)x3 (Supp. Figure S6A). FISH analysis with D8Z2 (green) for centromere 8 confirmed the chromosomal origin of marker (Supp. Figure S6B), while ring chromosome 4 and 11 were not observed. UPD of chromosome 8 was excluded by SNP data in normal copy regions. Informative SNPs located at the copy-number gain region suggested the maternal origin of the marker. Microsatellite analysis on the trio showed three allele peaks on the marker chromosome 8 region of the patient. Genotype of only informative microsatellite locus (D8S532) located on the duplicated site of chromosome 8 demonstrated maternal origin of sSMC8.a with an intenser band of maternal allele (Supp. Table S2).

Coverage analysis of chromosome 8 from NGS data, revealed a 13,4Mb duplication, chr8:40082798-53561524 which was assumed to constitute in marker 8 structure (Figure 6A), while we did not detect a large scale duplication in chromosome 4 and 11. The mean coverage is calculated as 59x for the duplicated region of chromosome 8 and 43.5x for normal copy region. Breakpoint analysis on the duplicated region demonstrated insertion of further two 217bp and 86bp length duplicated fragments located at chr8:55759348-55759565 (mean coverage of 59x) and chr8:60002688-60002774 (mean coverage of 68.6x), respectively. Sanger confirmation of

breakpoints demonstrated a non-disordered joining of three non-contiguous fragments: 8b (chr8:40082798-53561524), 8f (chr8:60002688-60002774) and 8d (chr8:55759348-55759565) (Supp. Figure S6C). Thus, according to the final interpretation of NGS data, sSMC8.a is a ring chromosome, as previously suggested by karyotype analysis, spanning from chr8:40082798 to chr8:53561524, where the ring closure junction involved joining of fragment 8f and fragment 8d (Figure 6B). Additionally, breakpoint cloning at the fusion junctions revealed small insertions of non-templated 16bp (chr8:53561524::chr8:60002688), 3bp (60002774::chr8:55759348) and 34bp (chr8:55759565::chr8:40082798) sequences (Supp. Figure S6C). BLAT analysis showed first 20bp (TCACCTTGCTTTTAGATCTG) of 34bp insertion had a 100% nucleotide similarity with chr7:40882523-40882542, a region encompassing intron 14 (NM\_001193311) of C7orf10. Microhomology of 2bp (CT) was detected at BPJ\_8b(+)\_8f(+). Loss of telomeric sequence provided further evidence for a ring shape of sSMC8.a (Figure 6C).

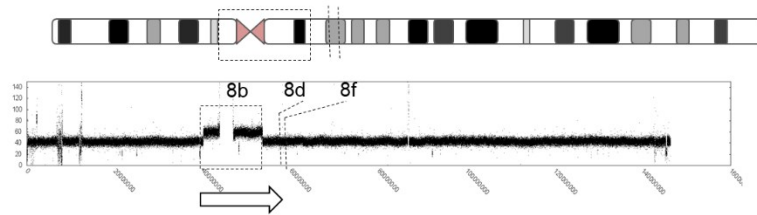
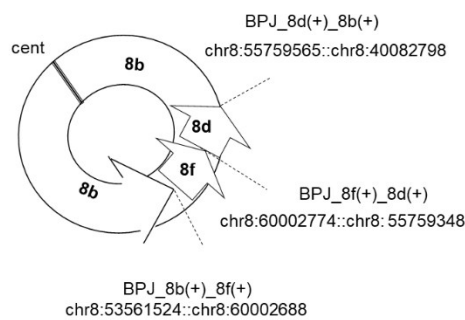
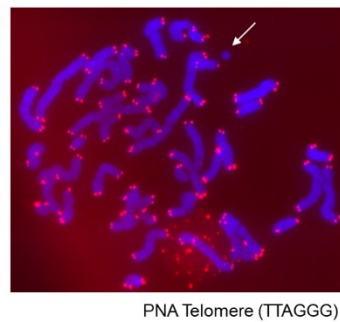
**A** sSMC8.a: chromosome 8**B****C**

Figure 6: (A) NGS coverage plot analysis of chromosome 8 revealed a 13.4Mb duplication, chr8:40082798-53561524 (fragment 8b). (B) Schematic illustration of the reconstruction of Ssmc8.a where the marker is a ring chromosome spanning from chr8:40082798 to chr8:53561524, where the ring closure junction involved joining of fragment 8f and fragment 8d (fragments not in scale). (C) FISH analysis by telomere-specific PNA telomeric probe demonstrated the absence of telomeric sequence on the marker chromosome (indicated by an arrow). For further details, see supplemental data (Supp. Figure S6)

**4.7 sSMC11**

Chorionic villus sampling is performed due to advanced maternal age. The ultrasound was initially normal but at the 11th week of gestation very mild decrease in growth parameters. sSMC in mosaic was detected and its presence is confirmed in amniotic fluid sampling (Supp. Figure S7A). CGH+SNP array performed in trio showed a *de novo* 9,1Mb pericentric duplication between 11p11.2 and 11q12.1 (Supp. Figure S7B). FISH

analysis with chromosome 11 centromere specific probe (D11Z1) confirmed the chromosomal origin of sSMC (Supp. Figure S7C). Ring shape of the marker is supported by the absence of telomere sequence on sSMC11 (Supp. Figure S7D). Informative SNPs at the copy-neutral region of chromosome 11 suggested biparental origin of the homologous chromosomes 11. Following microsatellite analysis with the probes targeting both duplicated and non-duplicated chromosome 11 regions demonstrated the maternal origin of sSMC11, showing the intenser band of the maternal alleles (Supp. Table S2).

NGS analysis performed on DNA extracted from amniotic liquid sampling revealed an unexpected complexity compared to the initial CGH array data. Coverage analysis of chromosome 11, from NGS data, revealed a several series of duplicated portions spanning from 11p15.5 to 11q12.1 with the mean coverage of 50.8x, while normal copy region is 38.9x. Discordant reads at the breakpoints of each copy number gain region, revealed a total of 14 fragments, where 13 were stitched together in a disordered pattern (Figure 7). The fragments are named as 11a, 11b, 11c, 11d, 11e, 11f, 11g, 11h1, 11h2, 11i, 11i2, 11j, 11k and 11l. . By Sanger sequencing we could solve 8 out of the 12 novel fusions (Supp. Figure S7E). The sequence characteristics at the junctions involved; up to 30bp insertions (4 junctions: BPJ\_11f(-)\_11g(+), BPJ\_11g(+)\_11a(+), BPJ\_11b(+)\_11d(+) and BPJ\_11d(+)\_11e(-)), blunt fusions (2 junctions: BPJ\_11a(+)\_11b(+) and BPJ\_11c(+)\_11j(-) and microhomology of 3bp and 8bp (2 junctions: BPJ\_11l(+)\_11h1(-) and BPJ\_11k(+)\_11i2(+)). In the four junctions with insertion only one junction, BPJ\_11f(-)\_11g(+), involved two templated insertions: 6bp insertion (chr11:34232223-34232229) and 30bp insertion

(Chr11:34232469-34232519), while the remaining three involved non-templated insertions.

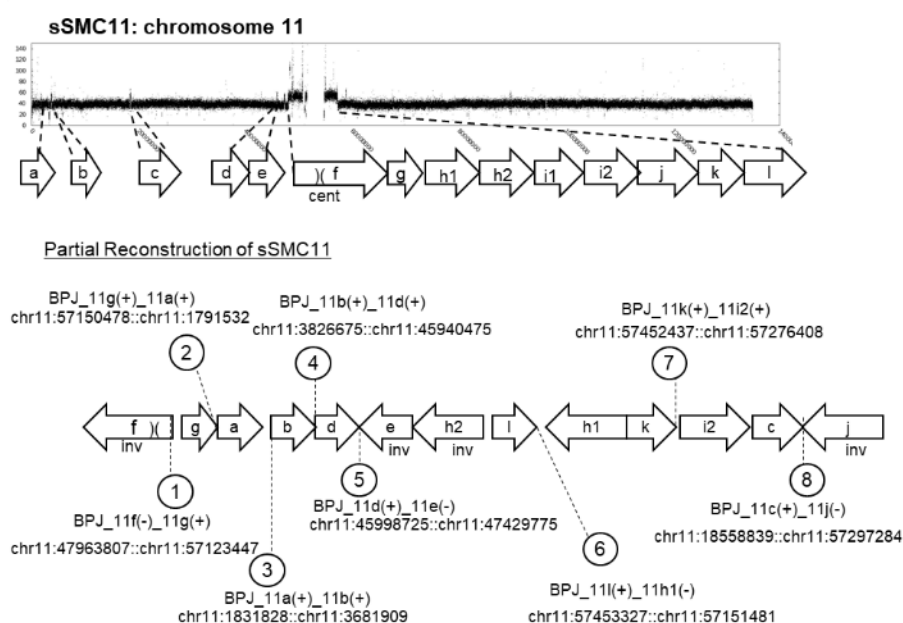


Figure 7: Coverage plot and breakpoint analysis of chromosome 11 by NGS data revealed a series of duplicated portions spanning from 11p15.5 to 11q12.1. Among the 14 duplicated fragments (11a, 11b, 11c, 11d, 11e, 11f, 11g, 11h1, 11h2, 11i, 11i2, 11j, 11k and 11l) 13 appear to be involved in the sSMC reconstruction with 4 inverted fragments (inv). Fusion junctions, validated by Sanger sequencing are indicated with numbers from 1 to 8 (fragments not in scale). For further details, see supplemental data (Supp. Figure S7).

#### 4.8 sSMC8.b

sSMC was detected in a child with severe psychomotor delay. The karyotype was described as 47,XX,+mar[20]/46,XX[10] where the marker chromosome was present in 66% of the cells. Following CGH+SNP array analysis revealed a de novo 46.7Mb duplication on chromosome 8 spanning from 8p23.1 to q12.1 (Supp. Figure S8A). UPD on chromosome 8 is excluded by SNP data. Informative SNPs located at the copy gain region

suggested a paternal origin of the marker chromosome 8. Microsatellite analysis on trio performed on duplicated and non-duplicated portions of chromosome 8 demonstrated a paternal origin of sSMC8 with an intenser band from paternal allele and biparental origin of corresponding homologous chromosome (Supp. Table S2). Coverage plots obtained from NGS data showed the duplicated portion of chr8:9770505-56539165 with the mean coverage of 80.12x. The mean coverage of 61.84x was calculated for the normal copy region (Supp. Figure S8B). Paired reads on the breakpoints of duplication suggested the fusion of up and down sites of duplication, possibly forming a ring structure. Sanger sequencing confirmed the ring fusion junction chr8:56539165::chr8:9770505 which involved microhomology of 7bp (AAATGAT) (Supp. Figure S8C).

#### 4.9 sSMC1

Karyotype analysis on PBL cells of a male patient with severe intellectual disability, microcephaly and mild aortic insufficiency detected a supernumerary chromosome in mosaic. CGH+SNP array in trio revealed a 15,9Mb de novo duplicated portion at the pericentromeric p21.1-p11.2 region of chromosome 1 of the patient (Supp. Figure S9A). Informative SNPs located at three loss of heterozygosity (LOH) regions, 1p36.33p34.3, 1p34.3p12 and 1q21.3q25.3, indicated a maternal iso-disomy. Outside the LOH region, informative SNPs indicated a maternal heterodisomy of chromosome 1. Even though microsatellite analysis in the duplicated and non-duplicated portion of chromosome 1 was inconclusive due to the uninformative marker allele intensities, no data were incompatible with a paternal origin of the marker (Supp. Table S2). FISH analysis by WCP for

chromosome 1 and CEP1 specific probe confirmed the chromosome 1 origin of the supernumerary marker chromosome. Coverage plot of whole chromosome 1 from NGS data revealed a single duplicated region at chr1:105714230-121494969 with the mean coverage of 62.18x, while the normal copy region had a mean coverage of 51.76x (Supp. Figure S9B). We detected discordant reads at chr1:105714230, mating with chr1:121494969, indicating a fusion between the edges of the duplicated region. The direction of the reads (both having same orientation) suggested an inversion rather than a simple fusion, unless this finding reflects the limitation of NGS analysis at complex regions such as the pericentromeric ones. Repetitive sequences at chr1:121494969 impeded the Sanger validation of the fusion junction.

#### **4.10 sSMC7.b**

Marker chromosome 7 was detected in a female child with the signs of Silver-Russel syndrome. Initial karyotype analysis revealed a supernumerary ring chromosome in 27 out of 30 examined metaphases. CGH+SNP array analysis on trio revealed a de novo duplication of a single region of chromosome 7, spanning from 7p22.1 to 7q11.23 (chr7: 6127453-73735597) (Supp. Figure S10A). Informative SNPs located at the three LOH copy-neutral regions, 7p21.2p14.3, 7q21.2q31.1 and q36.1q36.3, indicated a maternal uniparental disomy (UPD). Chromosomal origin of sSMC7.b was verified by the positive signal of the FISH probe D7Z1, targeting centromere 7, on marker chromosome (Supp. Figure S10B). Paternal origin of the marker is suggested by the informative SNPs located at the duplicated region of chromosome 7. Microsatellite analysis performed

with probes targeting duplicated and LOH region demonstrated a paternal origin of sMSC7.b and a maternal hetero/isodisomy of corresponding homologous chromosomes 7 (Supp. Table S2). Ring shape of sSMC7.b was demonstrated by the loss of telomere sequence on marker chromosome (Supp. Figure S10C). Coverage plots from paired-end WGS showed a single duplicated segment with the breakpoints of chr7:61792028-73750904 (Supp. Figure S10D). The mean coverage is calculated 63,8x for the duplicated region and 48,5x for the normal copy region. Similar to the sSMC1, the direction of the reads suggested an inversion. Because of high abundance of repetitive sequences at chr7:61792028, we could not yield a specific PCR product of the fusion junction.

#### 4.11 sSMC8.c

Karyotype analysis on PBL cells of 30 year-old health female detected a supernumerary chromosome in mosaic. CGH+SNP array in trio revealed three de novo duplications at the chromosome 8 of the patient; 8p11.22p11.1, 8q11.1q11.23 and 8q13.1q21.11 (Supp. Figure S11A). Informative SNPs in the duplicated region revealed a maternal origin of sSMC8, while the SNPs at the normal copy region demonstrated the biparental origin of the homologous chromosomes 8. Microsatellite analysis of the trio targeting the marker region was inconclusive (Supp. Table S2). Ring shape of sSMC8.c was demonstrated by the loss of telomere sequence on the marker chromosome (Supp. Figure S11B).

#### 4.12 sSMC7.c

This is a 5 year-old female patient with Silver-Russell syndrome detected with mosaicism regarding a cell line with a sSMC and a normal cell line: 46,XX[12](75%)/47,XX,+mar[4](25%). CGH+ SNP array revealed a UPD at two regions of chromosome 7, 7p21.1p14.3 and 7q36.2q36.3, and a mild increase ( $\log_2=0,145$ ) in the pericentric region of the chromosome 7 (chr7:54010055-63986785) (Supp. Figure S12A). Following FISH analysis with chromosome 7 specific centromeric probe demonstrated the chromosomal origin of the sSMC (Supp. Figure S12B). In order to better evaluate the duplicated region at the chromosome 7, we performed high resolution 1M array (Agilent). However, we could not obtain a significant increase in the target region at 1M array data ( $\log_2=0,08$ ). Ring shape of sSMC7.c was demonstrated by the loss of telomere sequence on marker chromosome (Supp. Figure S12C).

#### 4.13 Breakpoint Characteristics and Repeat Elements

Altogether, WGS revealed a total of 60 breakpoints within the duplicated regions (4 in sSMC18, 7 in sSMC2.a, 4 in sSMC2.b, 5 in sSMC7.a, 6 in sSMC17, 6 in sSMC8.a, 2 in sSMC8.b, 2 in sSMC7.b, 2 in sSMC1, 22 in sSMC11). We could fully characterize 19 fusion junctions of the duplicated fragments by PCR and Sanger sequencing (Table S3), which showed chromothripsis signatures such as blunt fusions (4: one in sSMC2.b and sSMC7.a, two in sSMC11), 2 to 8 bp microhomology (6: one in sSMC8.a, and sSMC8.b, two in sSMC11 and sSMC18), and 2 to 36 bp insertions (12: one in sSMC2.a, sSMC7.a and sSMC17, three in sSMC8.a, and six in sSMC11). Among the insertions, two were Line-1 elements (sSMC7a and

sSMC17) and two were small insertions coming from distal portions of the same chromosome (sSMC11), while the remaining ones were non-templated. In all but two cases (sSMC8.a and sSMC8b) the sSMC had one of the breakpoints falling within the centromeric alphoid sequences, which impaired the complete characterization of breakpoint sequences. In particular, in sSMC18 (Figure 1), Sanger sequencing of fusion junction, detected by NGS analysis, demonstrated the ring closure junction between chr18:49040431 and Alphoid DNA L1.84 of chromosome 18.

Overall, 62% (37 out of 60) of the breakpoints are enriched with repeat elements; satellites (4 breakpoints), line elements (7 breakpoints), Long-Terminal Repeats (LTR) (6 breakpoints), simple repeats (2 breakpoints), DNA repeats (4 breakpoints) and Alu repeats (14 breakpoints). Remarkably, we detected 13 out of 14 Alu elements in the case SMC11. Alu-Alu mediated recombination could be predicted for six fusion junctions; e-h2, h2-l, l-h1, h1-k, k-i2 and i2-c therefore explaining six out of eleven rearrangements detected in the marker chromosome case sSMC11 (Supp Figure S13A). In fusion junctions e-h2 and k-i2, Alu repeats having same orientation at both breakpoints showed 86% and 78% nucleotide match, respectively. In remaining fusion junctions between the fragments h2-l, l-h1, c-i2 and h1-k Alu repeats having opposite orientation at both breakpoints showed 84%, 82%, 76% and 76% nucleotide match, respectively. As previously reported (Nazaryan-Petersen et al., 2016), Alu/Alu mediated recombination could bring distal sequences at close proximity, therefore contributing to the formation of the chromothriptic rearrangement (Supp. Figure S13B). Among these Alu/Alu mediated rearrangements, we could validate only two of the junctions k-i2 and l-h1 (BPJ\_11k(+)\_11i2(+)) and

BPJ\_11l(+)\_11h1(-) by Sanger sequencing. The very case-specific pattern of this complex Alu/Alu mediated recombination is supported by the absence of the corresponding discordant reads in in-house WGS database (28 cases), excluding a possible SV call error due to sequence homology between the Alu.

#### **4.14 Disrupted-Fusion Genes**

Gene disruptions were detected in 29 out of 60 breakpoints, 28 of them occurring within introns while one was exonic (sSMC17). In sSMC18, *ROCK1* and *LINCO1630* were disrupted within intron 13 (NM\_005406.2) and intron 1 (NR\_040074.1), respectively. In sSMC2.a, *IL1R2* was disrupted within intron 1 (NM\_004633.3). In sSMC2.b, *FAM178B*, *NABI* and *DNER* were disrupted within intron 2 (NM\_016490), intron 6 (NM\_005966) and intron 9 (NM\_139072), respectively. In sSMC7.a, *ZNF735* was disrupted within intron 3 (NM\_001159524). Only in case sSMC11, one possible fusion gene was predicted as a result of fusion of two truncated genes (*PHF21A-SLC39A13*).

## 5. Discussion

Our study, brings together all previous observations, demonstrating by a whole cytogenomics approach that the primary driver for *de novo* sSMCs is a non-disjunction at the maternal meiosis followed by a partial trisomy rescue of the supernumerary chromosome present in the trisomic zygote, through chromothripsis-like processes. Trisomy, which is the most frequent chromosomal abnormality in humans and the leading cause of spontaneous abortions, is essentially linked to chromosome mis-segregation at the maternal meiosis with the risk for a trisomic conceptus increasing with the increase of maternal age (Nagaoka et al., 2012; Franasiak et al., 2014). Trisomy rescue, reported in no less than 1-2% of first trimester invasive prenatal diagnosis (Kalousek and Vekemans, 1996; Hahnemann and Vejerslev, 1997) and considered responsible for most false positive results by non-invasive prenatal screening (Hartwig et al., 2017), may save some of the embryos otherwise fated to be spontaneously aborted, leading to confined placental mosaicism where the abnormal cell line theoretically is isolated to the placenta and missing from amniotic cells or other fetal tissues. A probably less frequent phenomenon is a partial trisomy rescue in which only a part of the original trisomic chromosome is eliminated while a part remains, more often in the form of a supernumerary marker, in mosaic with a normal cell line. Cases in which the initial full trisomy could be documented by direct villus analysis with the subsequent partial correction leading to the presence of a sSMC are few (Srebniak et al., 2011; Vialard et al., 2009). More numerous are the cases in which the presence of the *de*

*novo* sSMC is accompanied by maternal hetero/isodisomy of the homologous chromosomes (Ahram et al., 2016; Liehr et al., 2015; Melo et al., 2015), a situation that can only be explained by a partial trisomic rescue of the supernumerary chromosome of paternal origin, after a non-disjunction event at the maternal MI. The same applies to those sSMCs in which three different haplotypes at the level of the marker chromosome and biparental origin of the SNPs along the normal homologs are detected, with the only difference that the trisomic rescue occurred on one of the two chromosomes of maternal origin. It is well known that anaphase lagging accounts for trisomy rescue of the supernumerary chromosome (Nicholson et al., 2015; Ly and Cleveland, 2017) which is then trapped within a micronucleus where massive shattering occurs (Zhang et al., 2015; Ly et al., 2016). As a consequence, the supernumerary chromosome is eliminated in one daughter cell, thus explaining the presence of the normal cell line. After the re-embedding of the micronuclear material into the main nucleus where DNA repair occurs (Ly et al., 2016), a second cell line containing a supernumerary chromothripsed chromosome would form, composed of only parts of the original supernumerary chromosome stitched together in a non-contiguous order. Depending on which of the three homologs undergo anaphase lagging, the remaining two may be in maternal hetero/isodisomy (loss of the paternal one) or of biparental origin (loss of one of the maternal ones). Trios genotyping in cases sSMC2.b, sSMC7a, sSMC7b, and sSMC1 detected maternal hetero/isodisomy of the normal homologs while the paternal origin of the sSMC could be demonstrated only in cases sSMC2.b, sSMC7.b, but was inconclusive in cases sSMC1 and sSMC7a. This condition fits with a maternal meiosis I (mat-MI) non-disjunction, followed

by chromothripsis of the supernumerary chromosome of paternal origin. Case sSMC8.a, with two different maternal haplotypes and a paternal one within the chromosome 8-derived sSMC region, and biparental SNPs along the two normal chromosomes 8, also indicates a mat-MI non-disjunction as the first event, in this case followed by chromothripsis of one of the chromosomes of maternal origin. In contrast, in cases sSMC18, sSMC2.a, sSMC17, and sSMC11, the marker region has the same haplotype as the intact maternally inherited chromosome, with biparental origin of the SNPs along the two homologous chromosomes. Since the markers we studied are from the pericentromeric regions of the respective chromosomes of origin, where cross-overs are not expected to occur, this finding indicates either a previous maternal meiosis II (mat-MII) nondisjunction or a postzygotic event. Indeed, in a number of cases of trisomy rescue (Chantot-Bastaraud et al., 2017) a mat-MII error has been documented. Similarly, the mechanism leading to the formation of the supernumerary i(12p), associated with Pallister-Killian syndrome, has been proven to be prezygotic and of maternal origin, presumably occurring at MII as demonstrated by the presence of three genotypes at the distal 12p region and only two at the pericentromeric one (Conlin et al., 2012; Blyth et al., 2015). The only case not compatible with a maternal meiotic non-disjunction is sSMC8.b, whose haplotype was paternal while the normal homologs were biparental. Thus, in this case we have to assume a postzygotic non-disjunction of the paternal chromosome 8, followed by chromothripsis of the supernumerary 8 and recovery of its pericentromeric region. Overall, the origin of the sSMC from a trisomy caused by maternal non-disjunction error at meiosis I, was directly demonstrated in four cases with hetero/iso UPD (sSMC2.b, sSMC7.a,

sSMC7.b and sSMC1) and in one case (sSMC8.a) with two maternal alleles on the marker region, while in five cases (sSMC18, sSMC2.a, sSMC17, sSMC11, sSMC8.c), the demonstration of a maternal meiotic error was indirect (Table 1). Remarkably, in all of these cases except for sSMC18 the maternal age at birth (Table 1) was increased (37.4 years on average), in agreement with a triggering event of maternal meiotic non-disjunction. WGS and breakpoint analysis by Sanger sequencing demonstrated that the sSMCs in 7 out of 10 cases, in addition to the pericentromeric region, contained one or more additional segments from their corresponding chromosomes, which were disordered assembled, a finding highly suggestive of a chromothripsis event. Notably, previous CGH or CGH+SNP array investigations had highlighted a non-contiguous constitution only in 4 of these cases. Breakpoint signature including blunt fusions, small insertions, microhomology in the fusion junctions of all cases indicated predominantly repair-based (NHEJ or alt-NHEJ) and replicative repair mechanisms (MMBIR).

**Table 1: Reconstruction and Formation Mechanisms of sSMC**

Case	mat age	Parental Origin		timing	sSMC construction	Breakpoint characteristics	Mechanism	Final interpretation
		sSMC	Hom. chr					
sSMC1	35	pat <sup>c</sup>	mat UPD (het/iso)	MI or post-zygotic	single fragment (15.7Mb)	Not validated		seq[GRCh37] +der(1) (p21.1->p11.2)
sSMC2.a	35	mat (single allele)	Biparental	MII or post-zygotic	4 fragments (2.7Mb+4.5Mb+ 254.6kb+ 704.7kb)/disordered	insertion 2bp (TA)	alt-NHEJ	seq[GRCh37] +der(2)(q11.1->q11.2::q12.2::q11.2->q12.1)
sSMC2.b	44	pat	mat UPD (het/iso)	MI	2 fragments (2.2Mb+ 38.7Mb)/disordered/ring	blunt fusion	NHEJ	seq[GRCh37] +r(2)::q11.1->q11.2::q32.2->q36.3::)
sSMC7.a	NA	pat <sup>c</sup>	mat UPD (het/iso)	MI	3 fragments (4.4Mb+ 1.2Mb/ 6.7kb)/disordered/ring	17bp insertion (LINE-1), blunt fusion	alt-NHEJ or MMBIR	seq[GRCh37] +r(7)::q11.21::p11.2->q11.21::)
sSMC7.b	39	Pat	mat UPD (het/iso)	MI	single fragment (12.4Mb)/Ring	Not validated		seq[GRCh37] +r(7)::p22.1->q11.23::)
sSMC7.c	38	NA	mat UPD	MI	single fragment (9.9Mb)/ring	Not involved in WGS		47,XX,+mar.arr[GRCh37] <sup>d</sup>
sSMC8.a	NA	mat (two alleles)	Biparental	MI	3 fragments (2.9Mb+4.4Mb/1.6Mb) disordered/ring	3bp, 16bp and 34bp of non-templated insertions and microhomology of 2bp	alt-NHEJ or MMBIR	seq[GRCh37] +r(8)::p11.21->q11.23::q12.1->q12::q12->q12::)

sSMC8.b	35	pat (single allele)	Biparental	post- zygotic	single fragment (46.7Mb)	microhomology of 7bp	alt-NHEJ or MMBIR	seq[GRCh37] +der(8)(p23.1- >q12.1)
sSMC8.c	33	mat	Biparental	MI or MII	3 fragments (4.4Mb+8Mb+6.7Mb)/ring	Not involved in WGS		47,XX,+mar.arr[G RCh37] <sup>d</sup>
sSMC11	39	mat (single allele)	Biparental	MII or post- zygotic	14 fragments (~9.1Mb in total) disordered/ring	6bp and 30bp templated insertions, 11bp, 13bp, 14bp and 30bp non- templated insertions, 2 blunt fusions, 3bp and 8bp microhomologie s	NHEJ/alt- NHEJ/MMBI RAlu-Alu mediated	seq[GRCh37] +r(11)::p11.2- >q12.1::q12.1::p15. 5::p15.4::p11.2::q1 2.1::)
sSMC17 <sup>a</sup>	39	mat (single allele)	Biparental	MII or post- zygotic	3 fragments/ disordered	36bp insertion (LINE-1)	alt-NHEJ	seq[GRCh37] +der(17)(q11.2::p1 1.2->q11.2::p11.2)
sSMC18 <sup>b</sup>	24	mat (single allele)	Biparental	MII or post- zygotic	2 fragments (74.4kb+7.5Mb) ordered/ring	microhomology of 4bp, microhomology of 4bp	alt-NHEJ or MMBIR	seq[GRCh37] +r(18)::q11.1::q12 .3->q21.2::)

The following abbreviations are used: NA (not available), Hom (homologous to the sSMC), chr (chromosome), mat (maternal), pat (paternal), UPD (uniparental disomy), MI (meiosis I), MII (meiosis II), NHEJ (non-homologous end

---

joining), alt-NHEJ (alternative NHEJ), MMBIR (microhomology mediated break induced replication), WGS (whole genome sequencing).

<sup>a</sup> Previously published case (Vetro et al. 2012)

<sup>b</sup> Previously published case (Rothlisberger 2000).

<sup>c</sup> Paternal origin of sSMC was assumed although microsatellite data were inconclusive.

<sup>d</sup> See Supp. Table S1 for the detailed description of array-CGH analysis

As a whole, our data show that the trigger for the formation of *de novo* non-recurrent sSMCs is a maternal meiotic non-disjunction followed by a post-zygotic chromothripsis event, due to anaphase lagging and repositioning of one of the trisomic chromosomes within a micronucleus. It seems probable that the formation of the new chromosome after the massive shattering that occurred in the micronucleus, depends on stochastic events, in the context however of some main limitations such as the propensity of the broken ends of the various fragments to integrate with each other, and the selection of more capable cells to survive and multiply in the presence of supernumerary chromosomal portions. Centric fragments should be easily preserved as sSMC (Figure 8), provided that they assume a ring conformation to compensate for the absence of telomeric sequences at both ends. Indeed FISH analysis in sSMC18, sSMC2.b, sSMC7.a, sSMC8.a, sSMC7.b, sSMC11, sSMC7.c, and sSMC8.c, whose small size made it impossible to understand if they were linear or circular structures, demonstrated the absence of the telomeric sequences, thus supporting their ring conformation. The preservation of supernumerary interstitial acentric fragments would require a neocentromerization event as indeed demonstrated in some sSMCs (Klein et al., 2012). The case reported by Kato et al., 2017 of a *de novo* interstitial translocation derived by chromothripsis of a supernumerary chromosome present in a trisomic zygote, demonstrates that acentric interstitial fragments may also be captured by another chromosome (Figure 8). Finally, chromothripped fragments equipped with both centromeric and telomeric sequences at one end only (Figure 8), may be stabilized provided that they capture a telomeric region from another chromosome, thus forming a *de novo* derivative supernumerary marker chromosome (cases 3 and 4 in Vetro et al., 2012).

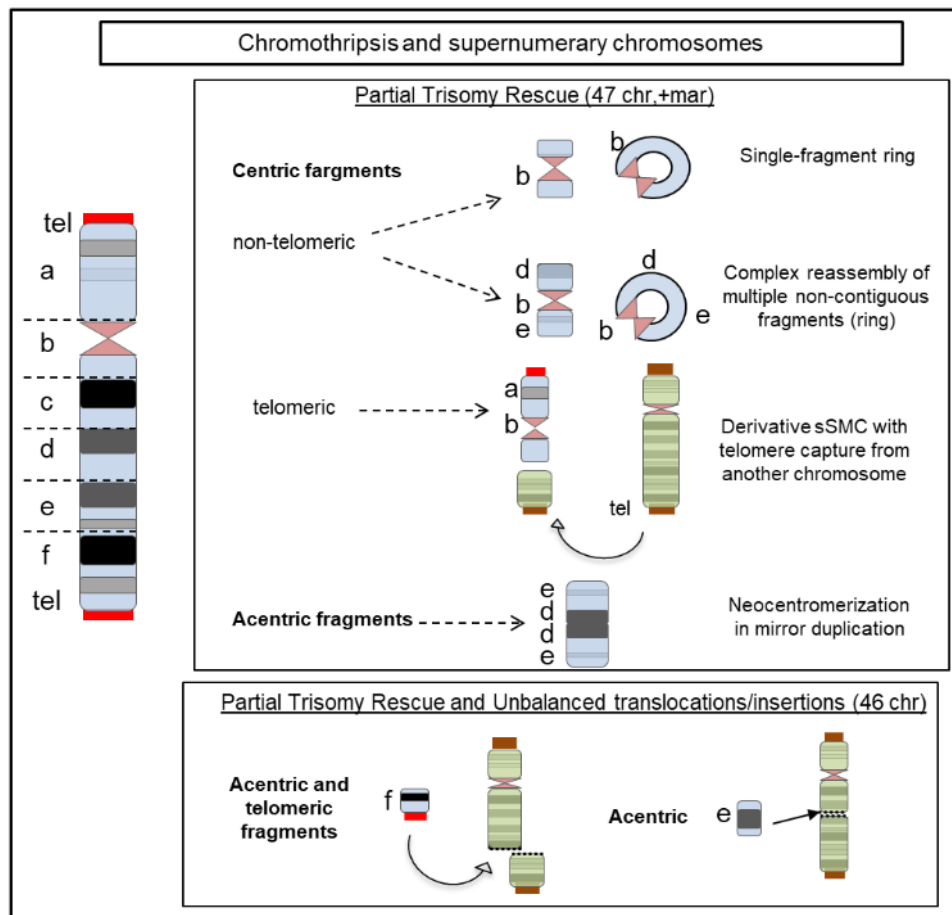


Figure 8: On the left, the hypothetical supernumerary chromosome shattered in a number of fragments (a, b, c, d, e, f) is depicted. Depending on which fragments of the original in-trisomy chromosome that are preserved and lost after chromothripsis, different types of rearrangements may be formed. Top box: centric fragments. Partial trisomy rescue leading to the formation of a supernumerary marker chromosome (mar). A supernumerary ring chromosome may form if at least one centric portion is present while both the telomeric ones (in red) are lost. A single fragment ring and a complex one, formed by non-contiguous fragments, are depicted. If both a centric and one telomeric portion (in red) are preserved, the chromothrised chromosome may acquire a second stabilizing telomeric region (in brown) from another chromosome, generating a derivative supernumerary chromosome, as reported in (Vetro et al., 2012). Acentric fragments: when the preserved fragment(s) does not contain a centromeric region, neocentromere formation, associated with a mirror duplication of the entire fragment, can stabilize the supernumerary marker. Lower box, left: an acentric fragment equipped with one telomeric portion is donated to a recipient chromosome that loses one of its distal regions, leading to the formation of an unbalanced translocation within a 46 chromosome karyotype. Right: acentric fragment(s) devoid of

---

telomeric sequences, may be inserted within another chromosome leading to an unbalanced insertion within a 46 chromosome karyotype.

In conclusion our findings give account of all the peculiarities associated with *de novo* sSMC: maternal meiotic non-disjunction, which is the prelude to the formation of the sSMC, explains the increased maternal age reported in most *de novo* cases; anaphase lagging of the supernumerary chromosome and its subsequent insertion within a micronucleus that segregates to one of the two daughter cells, accounts for the mosaic condition with a normal cell line and a second one containing the sSMC; maternal (segmental) UPD occurs whenever the partial trisomy rescue affects the chromosome of paternal origin; chromothripsis explains why some sSMCs are formed by non-contiguous regions of a given chromosome. This multiple-step mechanism underlying the formation of most non-recurrent *de novo* sSMCs identifies a link between numerical and structural chromosomal anomalies and indeed suggests investigating whether other structural anomalies such as some unbalanced *de novo* translocations and insertions may be the final result of a mechanism initiated by a trisomy, passing through the elimination of the supernumerary chromosome by anaphase lagging and subsequent chromothripsis, as already anticipated (Janssen et al., 2011; Kato et al., 2017). On the other hand, from the point of view of genetic counselling, the discovery of such a multiple-step mechanism reveals a bitter truth, that is that the prognosis for those sSMCs identified in prenatal diagnosis will be infeasible. Indeed within a chromosome formed by multiple pieces, disruption of higher-order chromatin organization such as topologically associating domains will occur (Spielmann et al., 2018). The final effect of altered gene dosage, potential for dysregulation and for

formation of new genes by gene fusion (Spielmann et al., 2018), all in a mosaic state, will be a highly problematic cocktail.

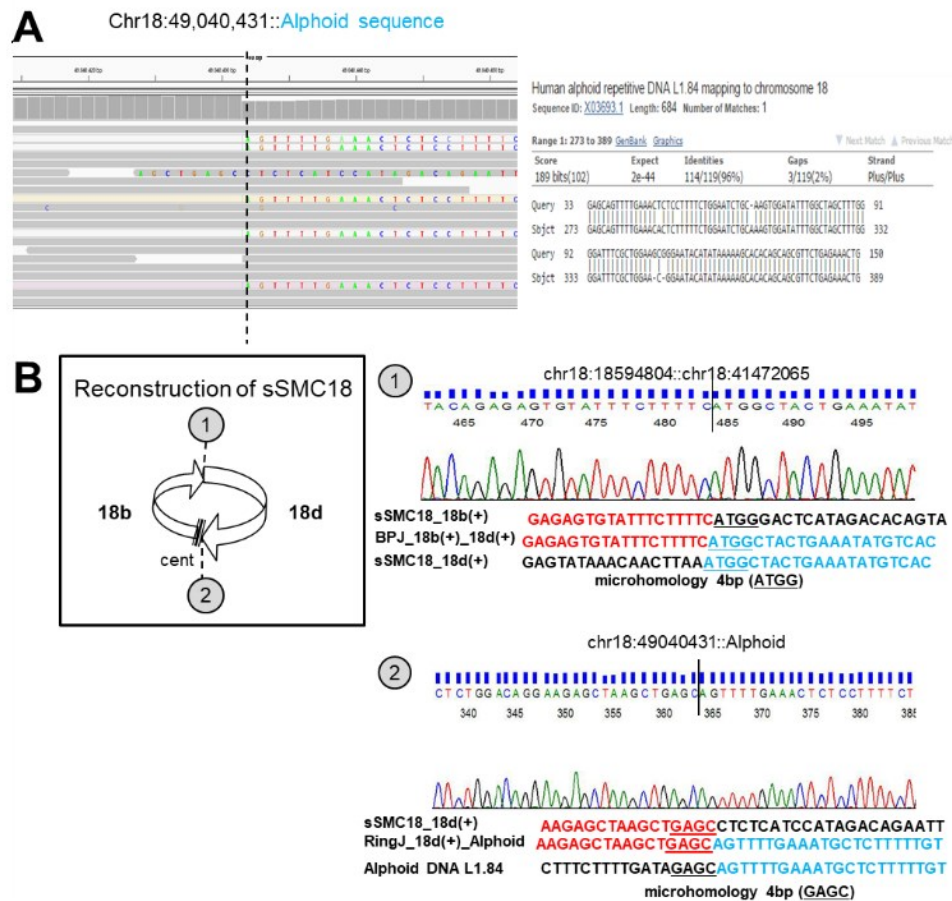
Trisomy rescue is likely to be the evolutionary trade-off to compensate for the massive loss of embryos caused by the high level of aneuploidy of human female gametes. However, the rarity with which the loss of the supernumerary chromosome is estimated to occur in healthy people (King et al., 2014; Robinson, 2000) indicates that this event, although providing a rescue from deleterious conditions, has no evolutionary advantage and reinforces the idea that meiotic non-disjunction in human females and the consequent aneuploidy leading to implantation failure and early miscarriage, is under Darwinian pressure. Indeed, by increasing the time between subsequent pregnancies, thus preserving the maternal resources, and by decreasing the likelihood of pregnancy in women too old to raise children (Wang et al., 2017; Warburton, 1987), the immense failure of aneuploidy pregnancies appears an optimal strategy to ensure the offspring of the attention and nourishment necessary for their survival and, not last, reduce the risk of dying from delivery haemorrhage. Noteworthy, the human life span from prehistory until 300 years ago was much shorter (Trinkaus, 2011), so women did not reach the menopause age and remained fertile until their death. On the other hand, most of the embryos carrying genetic defects secondary to total/partial trisomy rescue, either imprinting disorders, autosomal recessive diseases due to UPD, and supernumerary marker chromosomes for which a negative outcome is reported in 14-30% of the cases, appear able to get to the postnatal life, thus dissipating the benefits provided by the early loss of the conceptus. This may account for the limited evolutionary success of this mechanism.

## **6. Perspectives and future directions**

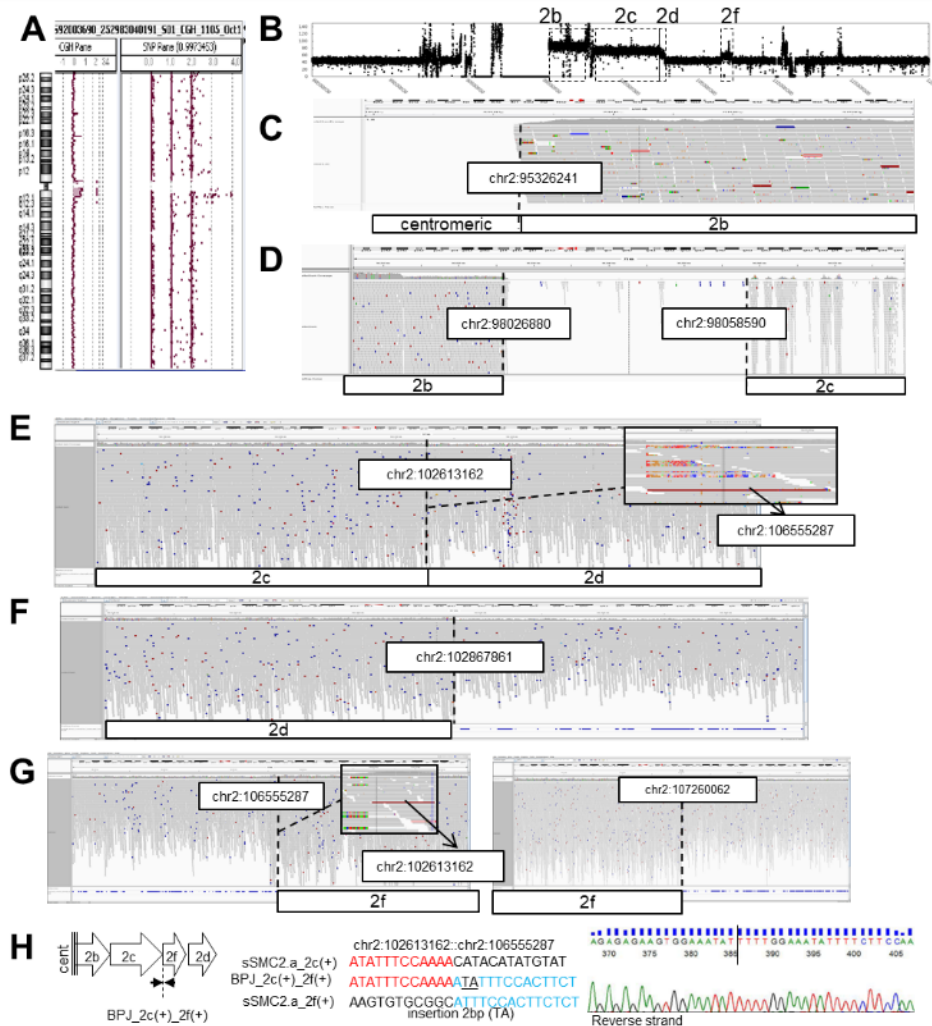
When we started this project, NGS application on a number of cases detected with sSMC was one of the first attempt at literature. Even though poor coverage at the centromeric regions embedded full genomic reconstruction of sSMC, our data revealed an unexpected structural complexity confined to extra chromosome of trisomy originated cells. Effect of sSMC on phenotype has been defined based only on the size and genetic content of sSMC (Marle et al., 2014). For this reason techniques like CGH+SNP array are accepted as gold standard to define pathogenicity of sSMC in due time of prenatal diagnosis. Our data suggests a new final effect of sSMC, expanding the pathogenicity definition of sSMC, where altered orientation of chromosomal portions may cause formation of new genes by gene fusion and gene expression dysregulation. Thus, even though high cost of NGS and lack of well trained technicians/researchers to cope with complex bioinformatics analyses cause a major limitation for everyday application of NGS in diagnostic laboratories, chromothripsis signatures detected in sSMC should be reflected on future studies aiming for a better genotype-phenotype correlation and more precise clinical diagnosis on patients with multiple abnormalities.

Mosaic condition of sSMCs still remained as a technical challenge to reconstruct sSMC by using paired-end WGS. Therefore, more sophisticated techniques like single-cell sequencing technologies (Liang et al., 2014) should be considered in next studies.

**Supplementary figures and tables**

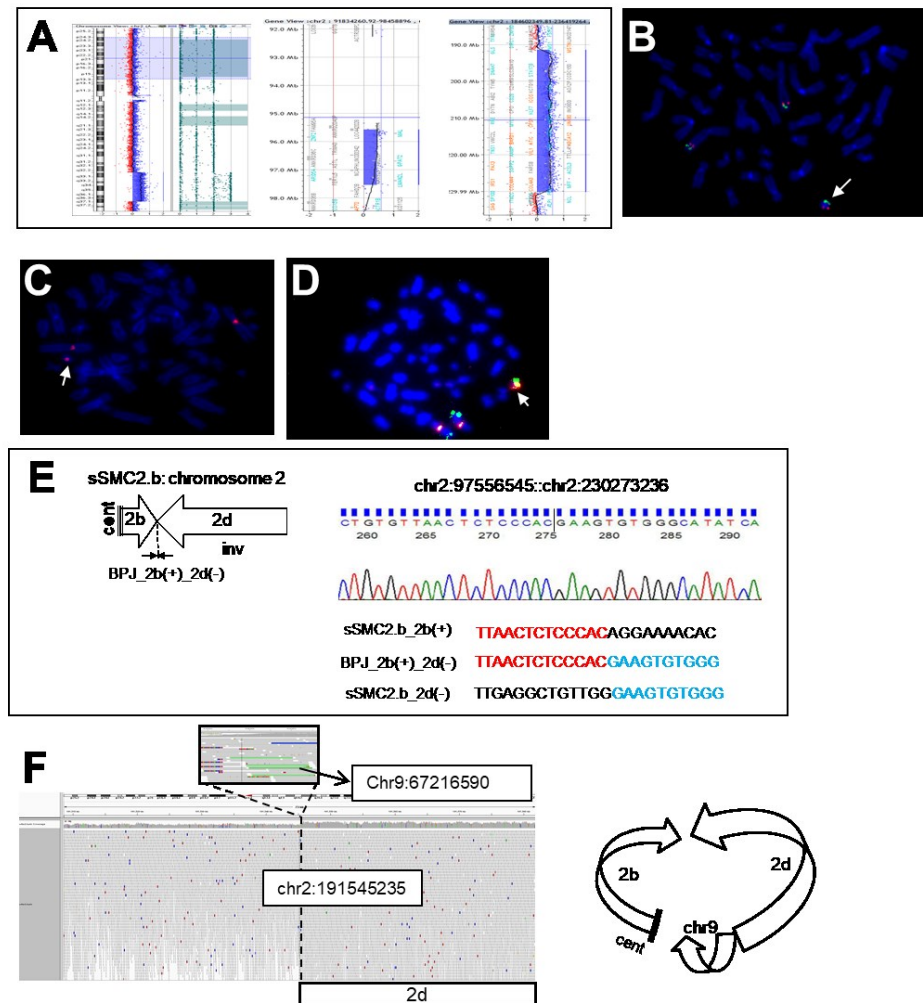


**Supplemental Figure S1:** (A) IGV view (integrative genomics viewer) and BLAST results of the discordant reads, from NGS data, at the distal end of the fragment 18d (chr18:49040431) which contains an 86bp sequence having 96% nucleotide match with human L1.84 alphoid repetitive DNA on chromosome 18, supporting a ring closure junction. (B) Schematic illustration of the reconstruction of sSMC18 and Sanger validation of fusion junctions at each end of the two duplicated fragments are shown. Reference sequences belonging to the duplicated fragments are indicated with red and blue. Microhomologies at the fusion junctions are underlined in the text. The breakpoint signatures indicated alternative non-homologous end joining (alt-NHEJ) with microhomology of 4bp (ATGG) at BPJ\_18b(+)\_18d(+) (number 1) and microhomology of 4bp (GAGC) at RingJ\_18d(+)\_Alphoid (number 2).

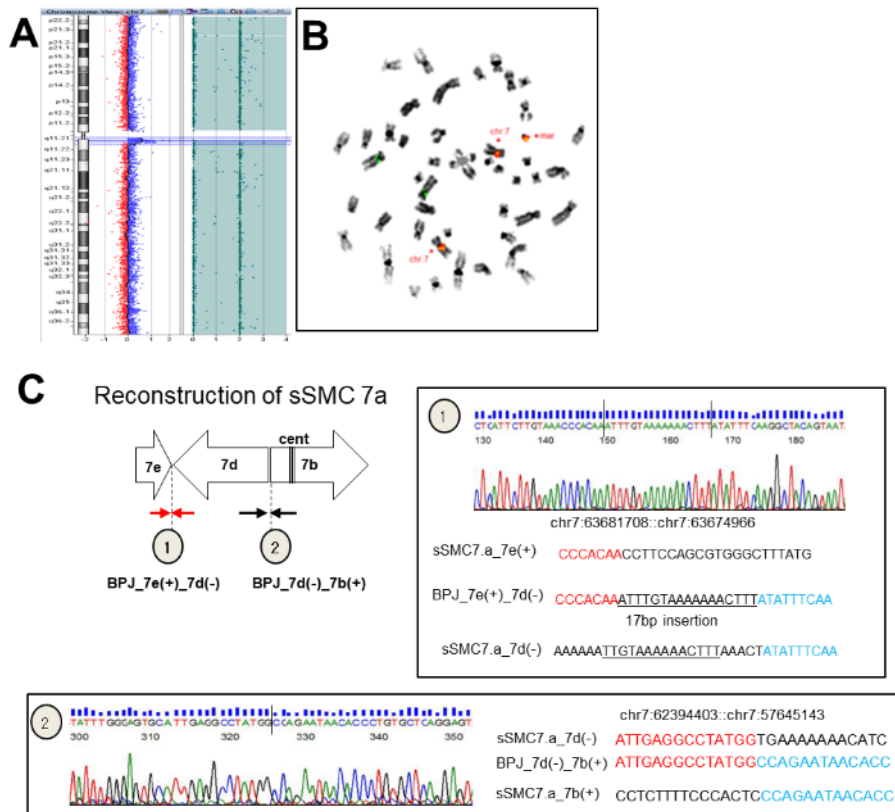


**Supplemental Figure S2:** (A) CGH+SNP array showed a *de novo* mosaic amplification of a region spanning from 2p11.2 to 2q12.1 (chr2:89143658-102866253) and a *de novo* duplication at 2q12.2 (chr2:106604839-107241592). CGH+SNP array in the trio suggested a biparental origin of the homologous chromosomes 2 and a maternal origin of the marker. Trio microsatellite analysis targeting the duplicated region confirmed the maternal origin of the marker with an intenser band of maternal allele. (B) Coverage plot analysis showing the sites of increased coverage at the pericentric region of the chromosome 2. Dashed lines indicate the borders of case specific duplicated fragments; 2b, 2c, 2d and 2f. (C,D) IGV view of the breakpoints of the duplicated segments. The start and end point of the first duplicated segment, fragment 2b (chr2:95326241-98026880), and start point of fragment 2c (chr2:98058590) are shown. The duplicated fragments were located in poorly covered regions and NGS analysis was limited to capture discordant reads to define the exact breakpoints. Thus, the breakpoints of duplications were defined only by the coverage

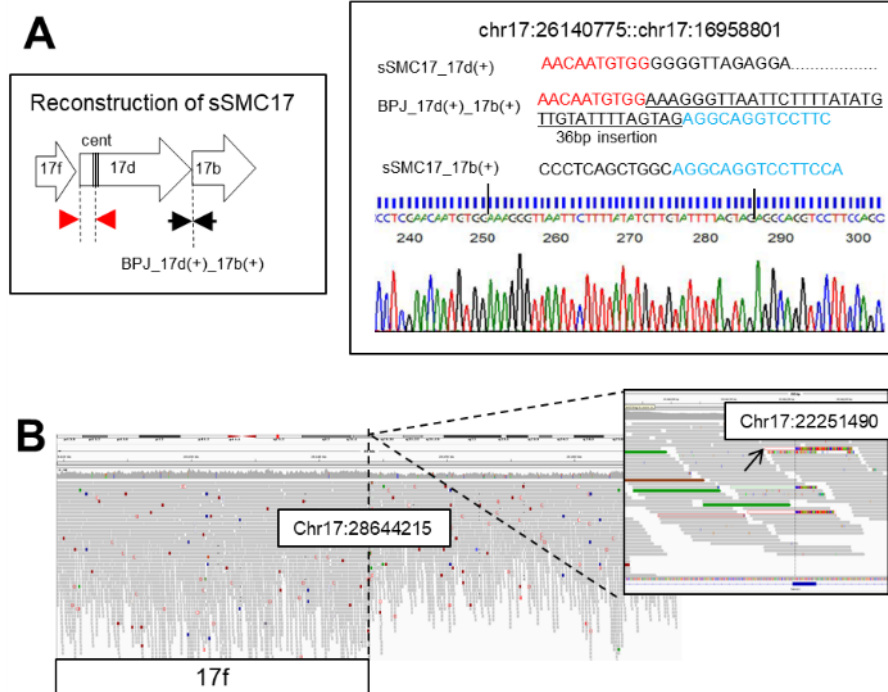
increase. (E) Discordant reads (see inset magnification), at the end site of the fragment 2c (chr2:102613162), were mapped to chr2:106555287 (start site of the fragment 2f). (F) End site of the fragment 2d (chr2:102867861) showing the change in the coverage. (G) Start (chr2:106555287) and end sites of the duplicated fragment 2f (chr2:107260062) were shown. Discordant reads at chr2:106555287 were mapped to chr2:102613162, thus indicating a disordered fusion of duplicated fragments 2c and 2f. (H) Sanger confirmation of the fusion junction between the fragments 2c and 2f, BPJ\_2c(+)\_2f(+) (chr2:102613162::chr2:106555287) is shown. Reference sequences belonging to the duplicated fragments are indicated with red and blue. We detected insertion of 2bp (TA) at 1bp downstream of the junction point. The inserted sequence is underlined in the text.



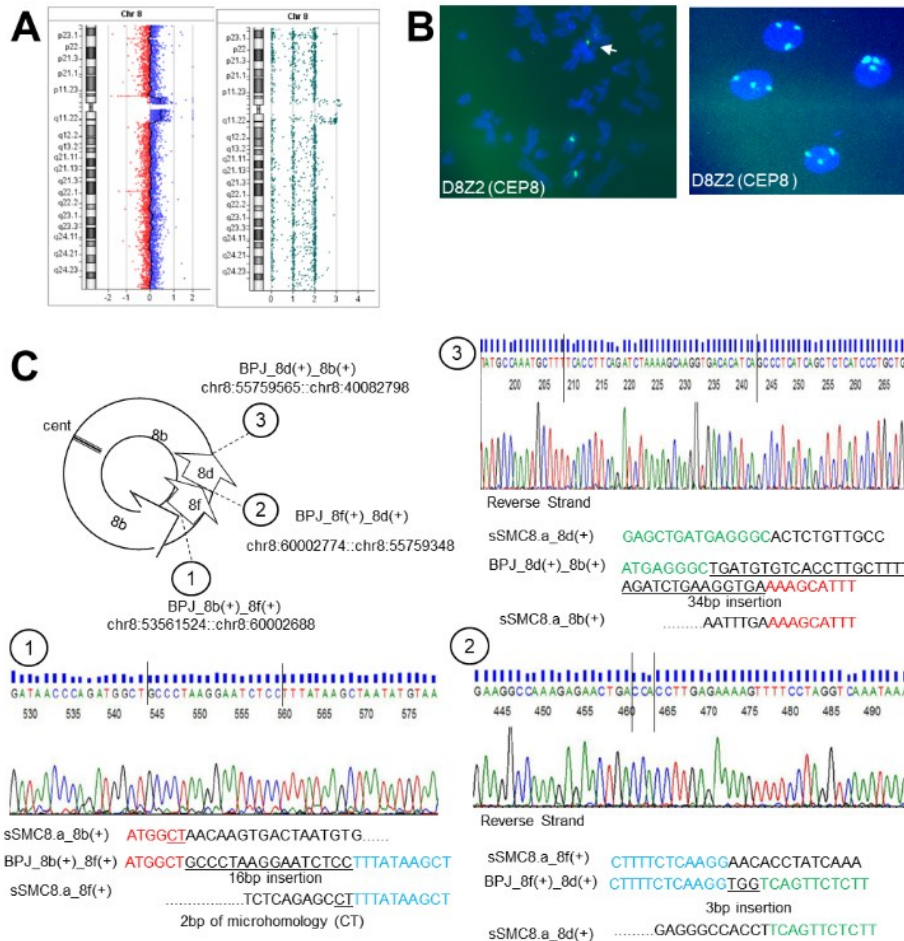
**Supplementary Figure S3:** (A) CGH+SNP array analysis of the fetal DNA revealed loss of heterozygosity (LOH) regions on chromosome 2 and two *de novo* non-contiguous duplications at 2q11.1q11.2 (chr2:95561604-97547601) and 2q32.2q36.3 (chr2:191482943-230254104), of 1.9Mb and 38.7Mb respectively. Informative SNPs along chromosomes 2 indicated a maternal hetero/isodisomy. Microsatellite analysis with probes targeting duplicated and copy-neutral regions confirmed the maternal heterodisomy and showed the paternal origin of the marker chromosome. (B, C, D) FISH analysis with probes targeting SATB2 (2q33.1, red), PAX3 (2q36.1, green) and D2Z1 (CEP2, red) confirmed the content of the sSMC2.b marker. The construction of sSMC2.b is also shown by the fusion of two FISH signals targeting fragment 2b (CEP2, red) and fragment 2d (PAX3, green). (E) Sanger sequencing of novel fusion junction BPJ\_2b(+)\_2d(-) (chr2:97556545::chr2:230273236) demonstrated a blunt fusion. (F) IGV view of the breakpoint at the start site of the fragment 2d, chr2:191545235, showing discordant reads mapping to chr9:67216590, suggesting an insertion from a genomic region belonging to chromosome 9 within a possibly ring sSMC2.b.



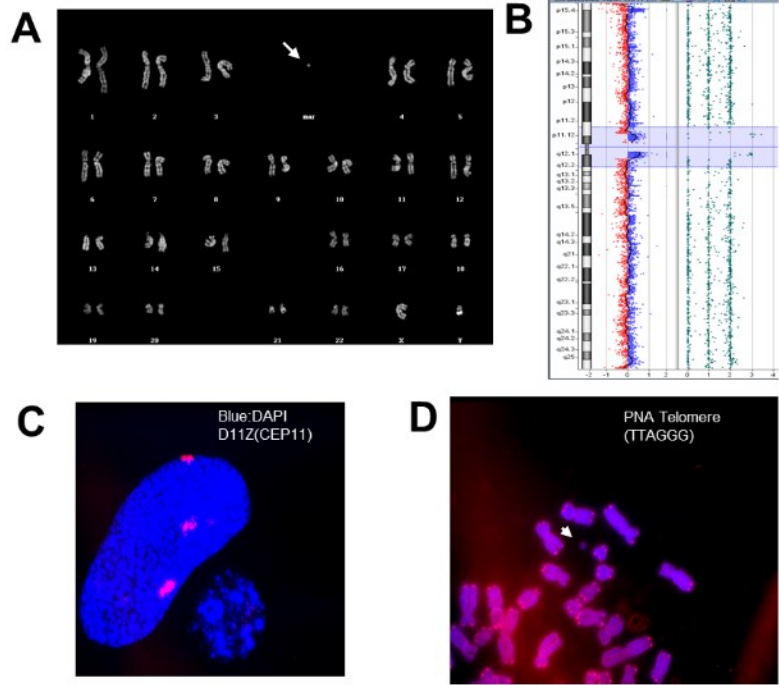
**Supplemental Figure S4:** (A) CGH+SNP array analysis of the patient's DNA revealed LOH at 98% of the SNPs on chromosome 7, indicative of uniparental isodisomy, and a single pericentromeric duplicated region 7p11.2.q11.21. Microsatellite analysis performed on the trio revealed a maternal isodisomy for microsatellite markers D7S524, D7S495 and D7S515; maternal heterodisomy in marker D7S502 (data not shown). (B) FISH analysis with BAC probes RP11-144H20 (chr7:61968709-62155949, red) targeting fragment 7b, RP11-340I6 (chr7:63271383-63465453, purple) and RP11-3N2 (chr7:63427818-63579385, yellow), both targeting fragment 7d, showed the presence of signals on the supernumerary marker chromosome (indicated with arrows). (C) The sequence characterization of fusion junctions by Sanger sequencing showed a 17bp insertion at the fusion junction at BPJ\_7e(+)\_7d(-) (number 1). BLAST analysis of insertion showed a 100% nucleotide match with a LINE-1 (L1ME4a) element mapped on chromosome 9. On the other hand, a portion of 17bp could be templated by the short sequence flanking the breakpoint (underlined in the text, sSMC7.a\_7d(-)). The junction BPJ\_7d(-)\_7b(+)(number 2) showed a blunt fusion.

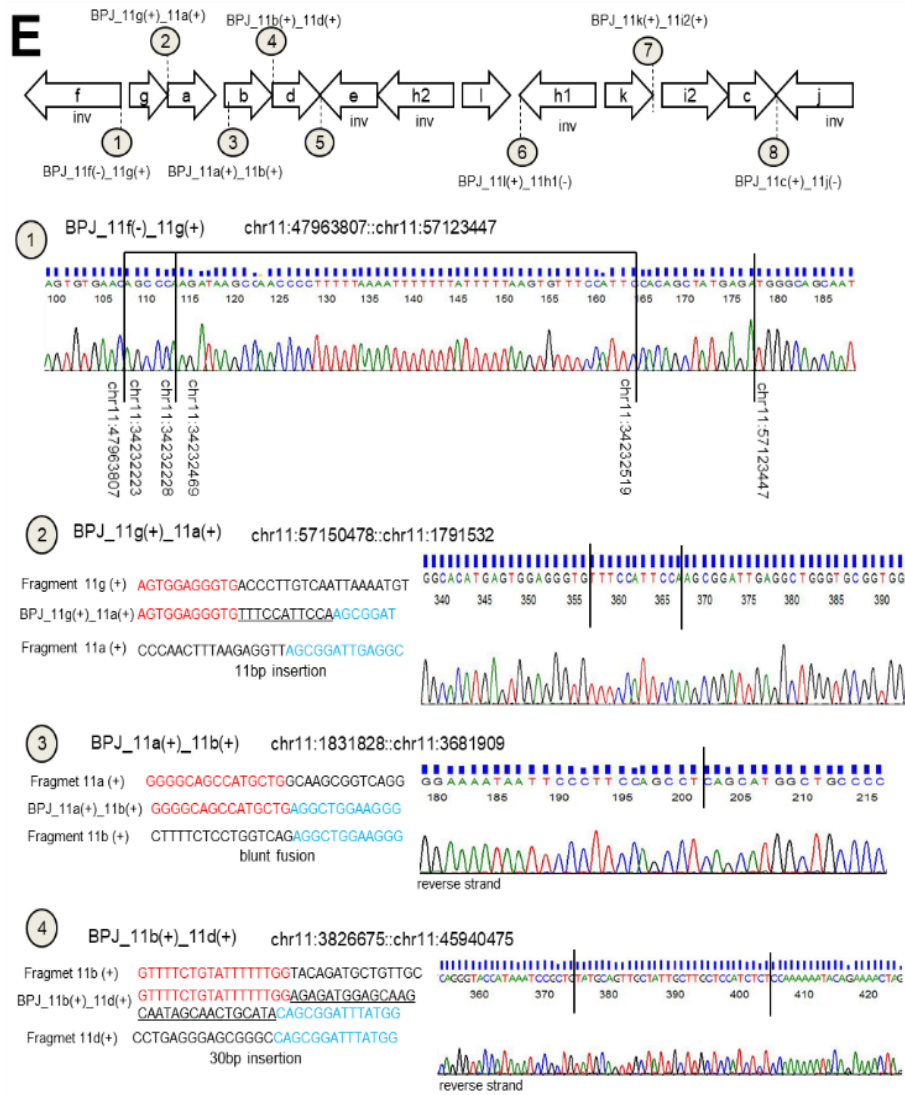


**Supplemental Figure S5:** (A) Sanger confirmation showed 36bp insertion (underlined in the text). BLAST analysis of insertion showed a 96% sequence match with LINE 1 (L1MB8) element. (B) IGV view of the breakpoint chr17:28644215, the end site of the third duplicated fragment 17f showing the discordant reads which are mapped to chromosome 17 centromeric region, chr17:22251490. Repeat elements at the centromeric site impeded the breakpoint cloning.



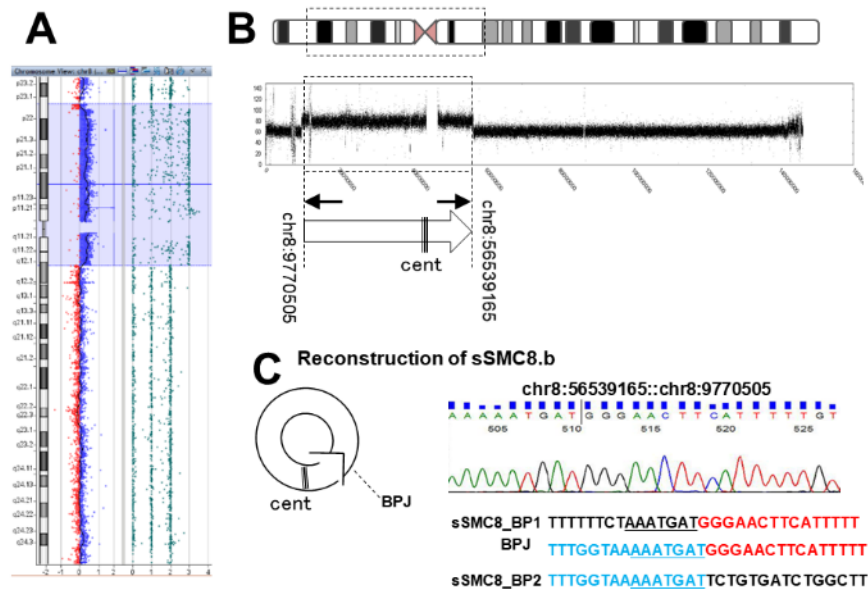
**Supplemental Figure S6:** (A) CGH+SNP array analysis revealing a *de novo* 13.4Mb pericentric duplication between 8p11.21 and 8p11.1. Uniparental disomy (UPD) of chromosome 8 was excluded by SNP data in the normal copy regions. Informative SNPs located at the copy-number gain region suggested the maternal origin of the marker. (B) FISH analysis with chromosome 8 centromere specific probe (D8Z2), confirming the chromosomal origin of the sSMC (indicated by an arrow). (C) Schematic illustration of the reconstruction of sSMC8.a and Sanger validation of ring closure junction. Reference sequences belonging to the duplicated fragments are indicated with red, blue, and green. Insertions and microhomology at the fusion junctions are underlined in the text. The disordered reassembly of three non-contiguous fragments, namely 8b (chr8:40082798-53561524), 8f (chr8:60002688-60002774) and 8d (chr8:55759348-55759565), was demonstrated. Small non-templated 16bp (number 1), 3bp (number 2), and 34bp (number 3) insertions were detected at the junctions. Microhomology of 2bp (CT) was detected at BPJ\_8b(+)\_8f(+). (number 1).



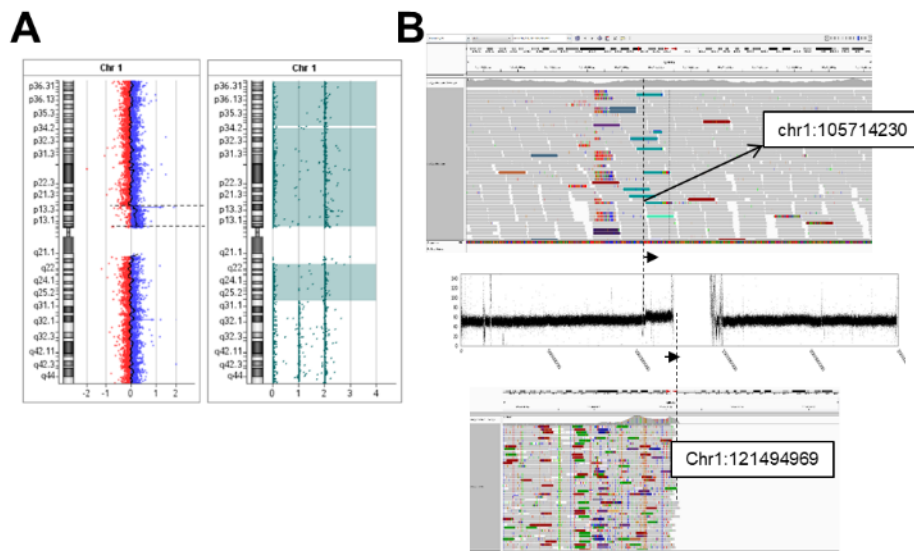




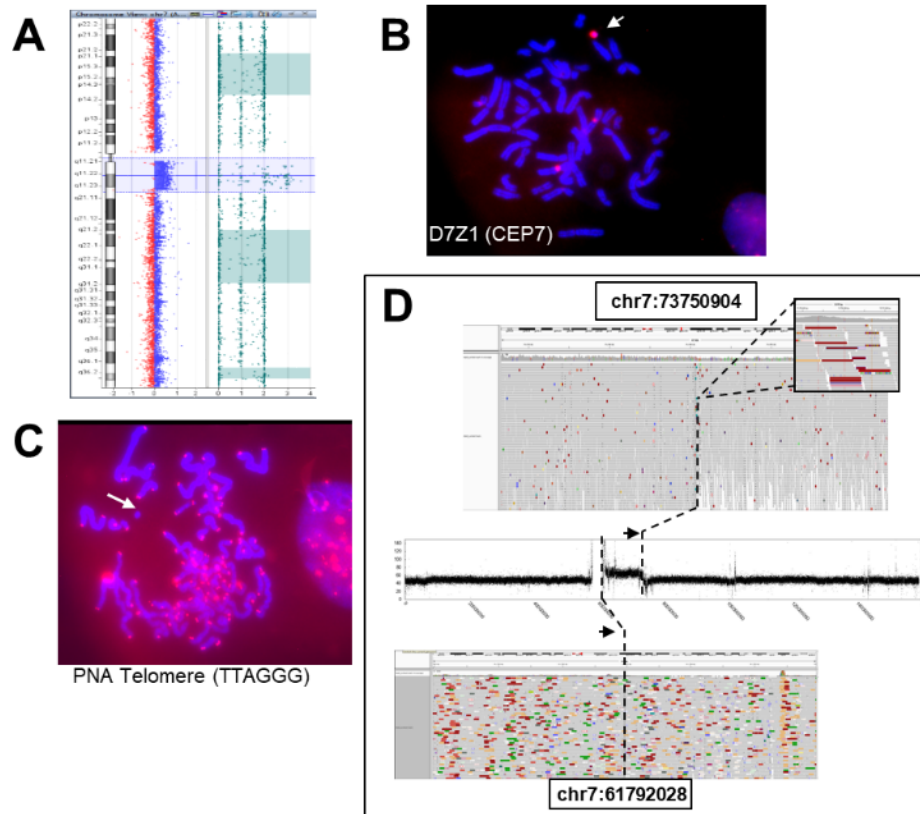
microhomology at the breakpoint junctions are underlined in the text. Reference sequences belonging to the duplicated fragments are indicated with red and blue. The breakpoints' signatures involved up to 30bp insertions (4 junctions: number 1, 2, 4 and 5), blunt fusions (2 junctions: number 3 and 8) and microhomology of 3bp and 8bp (2 junctions: number 6 and 7). The junction BPJ\_11f(-)\_11g(+) (number 1), involved 6bp (chr11:34232223-34232229) and 30bp (Chr11:34232469-34232519) templated insertions along with 13 bp non-templated insertion. The remaining three junctions (number 2, 4 and 5) involved non-templated insertions. At junction BPJ\_11l(+)\_11h1(-) (number 6), the sequences of fragment 11l and fragment 11h1 had imperfect sequence homology (nucleotide match between the fragments is illustrated with vertical bar '|'). In junction BPJ\_11k(+)\_11i2(+) (number 7), we detected the substitution of 2bp (g.57276415\_57276416GT>CT).



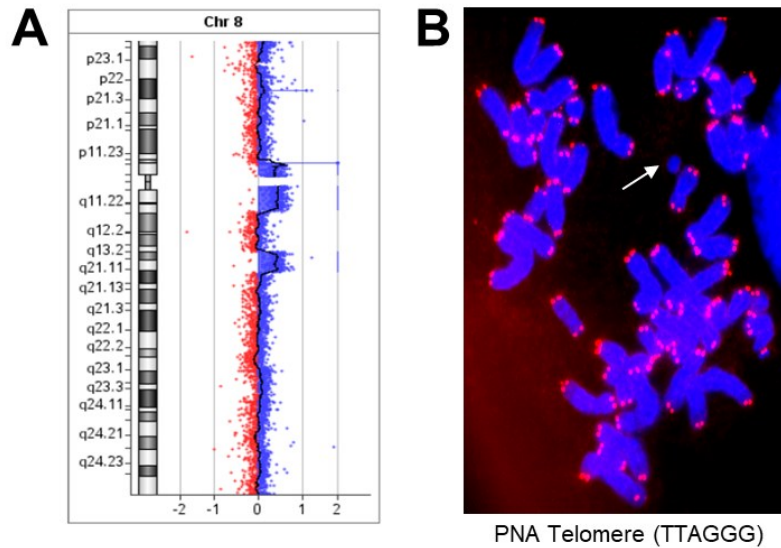
**Supplemental Figure S8:** (A) CGH+SNP array analysis revealed a *de novo* 46,7Mb duplication on chromosome 8 spanning from 8p23.1 to q12.1. (B) Coverage plot analysis of whole chromosome 8, from NGS data, showed a duplicated portion of chr8:9770505-56539165. Paired reads at duplication breakpoints (indicated with arrows) suggested the fusion of up and down sites of duplication, possibly forming a ring structure. (C) Schematic representation of ring sSMC8.b and Sanger sequencing confirmation of the ring fusion junction chr8:56539165::chr8:9770505 are shown. The fusion junction involved microhomology of 7bp (AAATGAT).



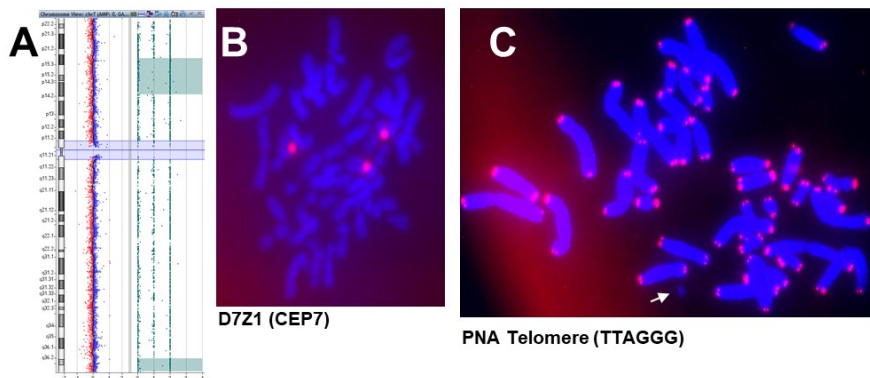
**Supplemental Figure S9:** (A) CGH+SNP array of the trio revealed a 15.9Mb de novo duplicated portion at 1p21.1-p11.2 in the patient. Informative SNPs located at three loss of heterozygosity (LOH) regions, 1p36.33p34.3, 1p34.3p12 and 1q21.3q25.3, indicated a maternal iso-disomy. (B) Coverage plot of whole chromosome 1 from NGS data, highlighting the duplicated portion. The IGV view of the breakpoints is shown. We detected discordant reads at chr1:105714230, mating with chr1:121494969, indicating a fusion between the edges of the duplicated region. Repetitive sequences at chr1:121494969 impeded the Sanger validation of the fusion junction.



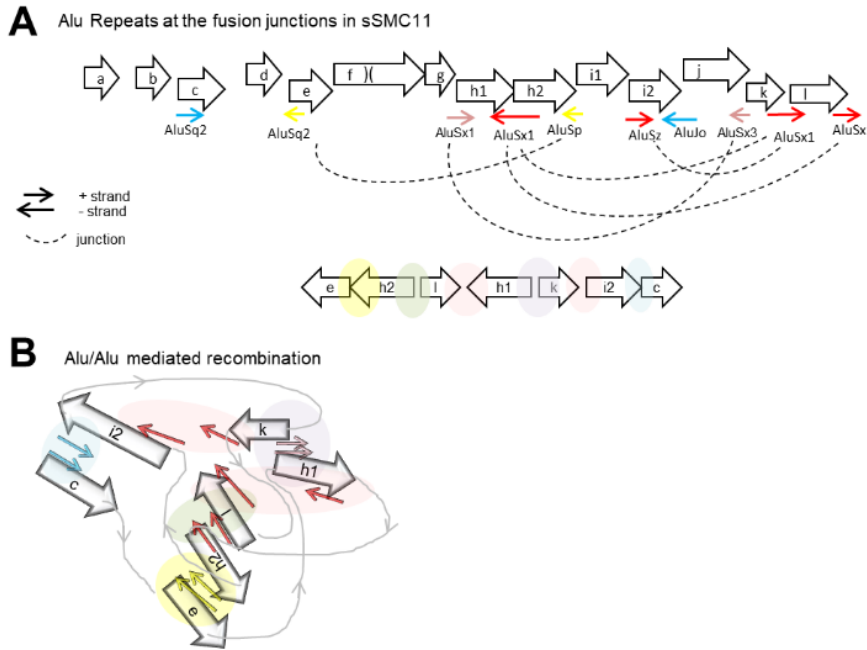
**Supplemental Figure S10:** (A) CGH+SNP array analysis of the trio revealed a de novo duplication of a single region of chromosome 7, spanning from 7p22.1 to 7q11.23 (chr7: 6127453-73735597). Informative SNPs located at the three LOH copy-neutral regions, 7p21.2p14.3, 7q21.2q31.1 and q36.1q36.3, indicated a maternal UPD. (B) Chromosomal origin of sSMC7.b was verified by the positive signal of the FISH probe D7Z1, targeting centromere 7, on marker chromosome. (C) FISH analysis by using telomere specific (TTAGGG) PNA probes showed the absence of telomere sequence in sSMC7.b. (D) Coverage plots from paired-end WGS showed a single duplicated segment with the breakpoints of chr7:61792028-73750904. Repetitive sequences at chr7:61792028 impeded the Sanger confirmation of the fusion junction.



**Supplemental Figure S11:** (A) CGH+SNP array of the trio revealed three *de novo* duplications within chromosome 8 in the patient: 8p11.22p11.1, 8q11.1q11.23 and 8q13.1q21.11. (B) FISH analysis by telomere specific (TTAGGG) PNA probes showed the absence of telomere sequence in sSMC8.b.



**Supplemental Figure S12:** CGH+SNP array revealed maternal hetero/isodisomy UPD at chromosome 7, 7p21.1p14.3 and 7q36.2q36.3, and a mild increase at chr7:54010055-63986785. (B) FISH analysis with chromosome 7 specific centromeric probe demonstrated the chromosomal origin of the sSMC. (C) FISH analysis by using telomere specific (TTAGGG) PNA probes showed the absence of telomere sequence in sSMC7.c.



**Supplemental Figure S13:** Schematic illustration of Alu repeats (shown as arrows), predicted to promote Alu/Alu-mediated recombination. We detected a total of 13 Alu elements at the duplication breakpoints. Depending on the sequence orientation of Alus, Alu/Alu mediated recombination could be predicted for six fusion junctions: e-h2, h2-l, l-h1, h1-k, k-i2 and i2-c, therefore explaining 6 out of the 11 rearrangements of the sSMC11. (B) Schematic representation of Alu/Alu mediated recombination bringing distal sequences at close proximity.

**Table S1: Karyotype&FISH and Microarray analysis**

Case ID	Karyotype& FISH	CGH+SNP Array (build 37/hg19)	Phenotype
sSMC 1	mos47,XY,+mar[20]/46,XY[80].ish der(1)(wcp1+,D1Z7+)	47,XX,+mar.upd(1)arr[GRCh37] 1p21.1q21.1(105427063-121330906)x2~3 dn 1p36.33p34.3(1089699_37707904) x2 hmz mat, 1p34.3p12(39557810_120133323)x 2 hmz mat, 1q21.3q25.3(151560153_181712003)x2 hmz mat	Developmental delay, microcephaly (19 years)
sSMC2. a	mos47,XX,+mar(51%)/48,XX,+2mar(37%)/46,XX,(12%)	47,XX,+mar.arr[GRCh37] 2p11.2q12.1(89143658_102866253) x3~4 dn, 2q12.2(106604839-107241592)x3 dn	Modest global psychomotor delay (1 year)
sSMC2. b	mos47,XX,+r[70%].ish der(2)(D2Z1+,SATB2+, PAX3+)	47,XX,+mar.upd(2).arr[GRCh37] 2q11.1q11.2(95561604_97547601) x3 dn htz, 2q32.2q36.3(191482943_230254104)x3 dn, 2p24.3p14(15099176_64802062)x2 hmz mat, 2q11.2q12.3(101132660_109960595)x2 hmz mat, 2q14.1q14.3(117225593_129663944)x2 hmz mat, 2q36.3q37.2(230202099_235743249)x2)x2 hmz mat, 2q37.2q37.3(236386804_241427162)x2 hmz mat	Fetal multiple malformations and termination of pregnancy
sSMC7. a	mos47,XX,+r[53]/46,XX[47] 47,XX,+mar.ish min(7)(;p11.2→q11.1:) (RP11-10F11+)	47,XX,+mar.upd(7).arr[GRCh37] 7p22.3p21.3(884743_10211892)x2 hmz, 7p21.3p11.2(10443341_57401695) x2 hmz, 7p11.2q11.21(57809849_63664030) x3 dn, 7q11.21q36.3(62509537_159030335)x2 hmz	pre- and postnatal growth-retardation; macrocephalus; macro cornea; Silver-Russel syndrome

sSMC7. b	mos47,XX,+mar[27]/46,XX[3]	47,XX,+mar.upd(7)arr[GRCh37] 7q11.1q11.23(61274531_73735597) x3 dn 7p21.2p14.3(15070803_33063197) x2 hmz mat, 7q21.2q31.1(91191512_114009385) x2 hmz mat, 7q36.1q36.3(150431977_155285135) x2 hmz mat,	Silver-Russell syndrome (2 years)
sSMC7. c	mos46,XX [12] (75%) /47,XX,+mar [4] (25%)	46,XX.arr[GRCh37] 7p21.1p14.3(18068091_34294555) x2 hmz 7q36.2q36.3(152807247_158572273) x2 hmz 7p11.2.q11.21(54010055_63986785) x2~3 dn	Silver-Russell syndrome (5 years)
sSMC8. a	mos49,XY,+3mar[13]/48,XY,+2mar[22]/47,XY,+mar[23]/46,XY[2] r(4)::p12→q12::r(8)::p11.21→q11.21::) r(11)::p11.12→q11.1::)	47,XX,+mar.arr[GRCh37] 8p11.21p11.1(40089168-53487330)x3 dn	Pierre-Robin-sequence, ventricular septum defect, patent foramen ovale, cryptochism, flaccid joints, gothic palate, umbilical hernia, at birth urinary tract infection
sSMC8. b	mos47,XX,+mar[20]/46,XX[10]	47,XX,+mar.arr[GRCh37] 8p23.1-q12.1(9803437_56519601)x3 dn	2-year-old child, psychomotor delay
sSMC8. c	mos47,XX,+mar[26]/46,XX[14]	47,XX,+mar.arr[GRCh37] 8p11.22p11.1(39222427x2,39258894_43708292)x3 dn htz, 8q11.1q11.23(46924418_54975693) x3 dn htz,  8q13.1q21.11(67950050x2,67986658_74700710)x3 dn htz	30 years old healthy female, increased nuchal translucency in the fetus
sSMC11	mos47,XY,+mar[13]/46,XY[1] AF mos47,XY,+mar[31]/46,XY[3] CV	47,XY,+mar.arr[GRCh37] 11p15.5p15.4(1996741_2953565)x2~3 dn htz, 11p11.2-q12.1(47997461_57139699)x3 dn htz	Very mild decrease in growth parameters at 20 weeks of gestation, voluntary termination of pregnancy

Supplementary figures and tables

sSMC17	mos47,XX,+mar[80%]. ish der(17)(D17Z1+,RP11- 403E9+,RP11-746M1-)	47,XY,+mar.arr[GRCh37] 17p11.2(16892427_19888467)x2~3 dn, 17q11.1 (22427573-23163556)x2~3 dn, 17q11.2(23848894-25676268)x2~3 dn 17p11.2.q11.2(16845458- 25917469)x2~3 dn	Mild dysmorphic features and severe developmental delay (2 years)
sSMC18	mos46,XX[30%]/47,X X,+mar[70%].rev ish der(18)(:p11.1→q11.1:: q12.3→q21.1:) dn	NA	Psychomotor retardation and dysmorphic features (13 years)

**Table S2: Microsatellite Genotyping**

STS marker	Locus/Target	Proband	Mother	Father	Interpretation
sSMC1					
D1S243	1p36.33/LOH	136.84	136,8/158,25	148,47/160,2	Maternal UPD-isodisomy
D1S2715	1q21.3/LOH	158.78	156,91/158,78	148.9	Maternal UPD-isodisomy
chr1STS1	p13.2/DUP	174.88	161,86/174,9	174.89	not conclusive
chr1STS4	p13.1/DUP	246.24	239,9/246,18	242,09/246,24	not conclusive
chr1STS7	p13.2/DUP	156.92	156,63/165,29	156.53	not conclusive
chr1STS8	p13.1/DUP	311.46	301,02/311,51	311.54	not conclusive
sSMC2.a					
D2S2311	2q11.2/DUP	<b>146,79</b> /151,1	146,87/151,1	148,85/151,1	Maternal sSMC2
D2S2175	2q11.2/DUP	121.48	121.48	121.41	not conclusive
D2S2222	2q11.2/DUP	215,58/ <b>219,31</b>	219.31	215,58/221,29	Maternal sSMC2
sSMC2.b					
STS2	2q33.1/DUP	<b>185,06</b> /180.81	180.91/185.16	185.6/187.2	Paternal sSMC2
D2S72	2q33.2/DUP	156,79/158,8/ 160,92	156,8/160,91	158,5/161,01	Maternal UPD-heterodisomy and paternal sSMC 2
D2S2382	2q35/DUP	248,01/253,74/257,6	247,85/253,7	257.49	Maternal UPD-heterodisomy and paternal sSMC 2
D2S298	2q22.3/NORMAL	131.07/137.06	131.19/137.07	129.01/131.17	compatible with maternal UPD-heterodisomy
D2S93	2q24.1/NORMAL	147.79/167.48	147.87/167.4	158.62/160.61	Maternal UPD-heterodisomy
D2S142	2q24.1/NORMAL	257.4/ 259.26	257.31/259.17	257.03/259.07	not conclusive
D2S2305	2p21/LOH	<b>125,31</b>	125.22	121.29	Maternal UPD
D2S2369	2p21/LOH	241.14	241,14/246,74	246,96/252,46	Maternal UPD-isodisomy
D2S2254	2q14.2/LOH	181,06/194,67	181,06/194,67	194,81/212,15	compatible with maternal UPD-heterodisomy
D2S1356	2p21/LOH	234.01	234,4/249,44	249.26	Maternal UPD-isodisomy
sSMC7.a					
D7S3106	7p11.2/DUP	199.79	NA	199.89	not conclusive
D7S1945	7q11.21/DUP	185,38/ <b>199,78</b>	NA	199.78	supportive for paternal origin of the marker
sSMC7.b					

Supplementary figures and tables

D7S2429	7q11.21/DUP	175.19	175.08	175.08	not conclusive
D7S613	7q11.23/DUP	110,38/114,47/122,8	110,31/122,8	110,26/114,42	Paternal sSMC7
D7S1816	7q11.22/DUP	225,0/233,3/237,5	224,95/233,36	229,11/237,53	Maternal UPD-heterodisomy and paternal sSMC7
D7S3070	7q36.1/LOH	194.71	194,87/203,07	190,7/203,07	Maternal UPD-isodisomy
D7S2462	7q36.2/LOH	124.54	124,23/132,24	134.04	Maternal UPD-isodisomy
D7S2439	7q36.1/LOH	198.3	198,31/207,91	194,46/200,29	Maternal UPD-isodisomy
D7S2456	7q31.1/LOH	242,2/ 244,09	242,19/244,17	242,17/244,15	not conclusive
D7S2476	7q11.23/LOH	146,11/151,81	146,06/151,83	146.12	compatible with maternal UPD-heteroisodisomy
D7S799	7q31.1/LOH	130.41	130.62	130.64	not conclusive
<b>sSMC8.a</b>					
D8S532	8p11.21/DUP	<b>241,53</b> /245,38	241.53	237,61/245,47	Maternal sSMC8
D8S587	8q11.21/DUP	<b>178,51</b> /186,82	178,61/186,85	178.32	not conclusive
D8S1773	8q11.22/DUP	154,67/ <b>156,6</b>	154,67/156,51	154,67/156,42	not conclusive
D8S1110	8q11.23/DUP	259,82/275,9/280,0	259,91/280,09	276,01/280,09	Three peaks and compatible with Maternal sSMC8
D8S1104	8p11.21/DUP	125,3/129,54/137,6	125,34/129,54	125,34/137,6	Three peaks and compatible with Maternal sSMC8
D8S1012	8q11.21/DUP	422,49/459,08/462,88	458,96/462,65	422,37/430,2	Three peaks and compatible with Maternal sSMC8
<b>sSMC8.b</b>					
D8S255	8p11.21/DUP	<b>123,62</b> /119.6	113.14/123.6	119.64/123.52	Paternal sSMC8
D8S258	8p21.3/DUP	<b>143,39</b> /147.99	148.18	143.27	Paternal sSMC8
D8S1694	8q24.11/NORMAL	242,45/246,21	242.44	246.37	Biparental
D8S256	8q24.22/NORMAL	210,07/223,34	223,37/227,22	210,08/225,38	Biparental
D8S264	8p23.3/NORMAL	123,22/138,77	138.77	123,15/129,02	Biparental
D8S518	8p23.2/NORMAL	228,77/250,28	228,46/244,5	228,58/250,23	not conclusive
D8S1819	8p23.3 /NORMAL	202,8/218,33	202,99/218,43	203,94/218,42	Biparental
<b>sSMC8.c</b>					
D8S255	8p11.21/DUP	102.87/ <b>119,44</b>	102.85/119.44	102.86/119.44	not conclusive
D8S532	8p11.21/DUP	251.38	245.51/251.29	241.69/251.38	not conclusive
D8S283	8p12/DUP	114.64	114.75	114.58/122.77	not conclusive
D8S1104	8p11.21/DUP	125.46	125.74/129.85	125.55/137.91	not conclusive
D8S587	8q11.21/DUP	170.4/ <b>186,97</b>	182.87/186.85	170.42/174.6	intense allele is not clear, but maternal allele was elevated by 20%

*Supplementary figures and tables*

sSMC11					
D11S1920	11q11/DUP	276,42/ <b>280,09</b>	280.09	276,42/280,38	not conclusive
D11S1978	11p11.2/DUP	<b>268,97</b> /284,15	269,24/288,1	273,08/284,19	Maternal sSMC11
D11S2005	11q12.1/DUP	<b>316,05</b> /320,0	316,15/324,33	320,1/324,33	Maternal sSMC11
D11S2016	11p11.2/DUP	291,49/ <b>295,51</b>	287,46/295,51	291,49/295,51	not conclusive
D11S1883	11q12.3/NORMAL	250,29/261,9	246,49/261,9	246,48/250,34	Biparental
sSMC17					
D17S916	17q23.1/NORMAL	262.59/266.493	247.41/266.6	262.93/294.68	Biparental
D17S1871	17p11.2/NORMAL	173.15/201.57	169.26/201.57	173.13/203.43	Biparental

Intenser alleles are given in bold.

**Table S3: Genomic Construction of sSMC by WGS**

Case	Whole Genome Sequencing					PCR&Sanger Sequencing	Reconstruction of sSMC
	Fragment ID	Genomic Location (hg19)	Cytoband	Size	Copy number	Sequence characteristics at fusion junction	
sSMC1	sSMC1	chr1:105714230-121494969	1p21.1.p11.2	15,7 Mb	Dup	Not validated	seq[GRCh37] +der(1) (p21.1->p11.2) chr1:g[105714230::121494969] add
sSMC2.a	sSMC2.a_2b	chr2:95326241-98,026,880	2q11.1.q11.2	2,7 Mb	Amp	BPJ_2c(+)_2f(+):insertion 2bp (TA)	seq[GRCh37] +der(2) (q11.1->q11.2::q12.2::q11.2->q12.1) chr2:g.[cen_95326241~_98026880~::98058590~_102613162::106555287::TA::106555288_107260062~::chr2:102613163~_102867861~]add
	sSMC2.a_2c	chr2:98,058,590-102,613,162	2q11.2	4,5 Mb	Dup		
	sSMC2.a_2d	chr2:102,613,163-102,867,861	2q11.2.q12.1	254,6kb	Dup		
	sSMC2.a_2f	chr2:106,555,287-107,260,062	2q12.2	704,7kb	Dup		
sSMC2.b	sSMC2.b_2b	chr2:95,326,171-97,556,545	2q11.1.q11.2	2,2 Mb	Dup	BPJ_2b(+)_2d(-):blunt fusion	seq[GRCh37] +r(2) (::q11.1->q11.2::q32.2->q36.3::) chr2:g.[cen_95326171_9755654

	sSMC2.b _2d	chr2:191,545,235- 230,273,236	2q32.2.q36 .3	38,7 Mb	Dup		5::191545235_230273236inv]a dd
sSMC7.a	sSMC7.a _7b	chr7:57,645,143- 62,050,000	7p11.2.q11 .21	4,4 Mb	Dup	BPJ_7e(+)_7d(-):17bp insertion (LINE-1) BPJ_7d(-)_7b(+):blunt fusion	seq[GRCh37] +r(7) (::q11.21::p11.2->q11.21::) chr7:g.[63674966~_63681708:: ATTTGTAAAAAACTTT::62 394403_63674966inv::5764514 3_cen_62050000~]add
	sSMC7.a _7d	chr7:62,394,403- 63,674,966	7q11.21	1,2 Mb	Dup		
	sSMC7.a _7e	chr7:63,674,967- 63,681,708	7q11.21	6,7k	Dup		
sSMC7. b	sSMC7.b	chr7:61792028- 73750904	7p22.1.q11 .23	12,4 Mb	Dup	Not validated	seq[GRCh37] +r(7) (::p22.1- >q11.23::) chr7:g[pter_61792028del::7375 0904_qterdel]add
sSMC8.a	sSMC8.a _8b	chr8:40082798- 53561524	8p11.21.q1 1.23	13,4 Mb	Dup	BPJ_8b(+)_8f(+):16bp non- templated insertion, microhomology of 2bp (CT) BPJ_8f(+)_8d(+):3bp non- templated insertion, BPJ_8d(+)_8b(+):34bp non- templated insertion	seq[GRCh37] +r(8) (::p11.21- >q11.23::q12.1->q12::q12- >q12::) chr8:g[53561524::GCCCTAAG GAATCTCC::60002688_60002 774::TGG::55759348_5575956 5::TGATGTGTCACCTTGCTT TTAGATCTGAAGGTGA::400 82798]add
	sSMC8.a _8d	chr8:55759348- 55759565	8q12.1	217 bp	Dup		
	sSMC8.a _8f	chr8:60002688- 60002774	8q12.1	86b p	Dup		

Supplementary figures and tables

sSMC8.b	sSMC8.b	chr8:9770505-56539165	8p23.1.q12.1	46,7 Mb	Dup	microhomology of 7bp (AAATGAT)	seq[GRCh37] +der(8) (p23.1->q12.1) chr8:g[9770505::56539165]add
sSMC11	sSMC11_11a	chr11:1791532-1831828	p15.5	40kb	Dup	BPJ_11f(-)_11g(+): 6bp templated insertion (chr11:34232223-34232228), 30bp templated insertion (Chr11:34232469-34232519) and 13 bp nontemplated insertion	seq[GRCh37] +r(11) (:p11.2->q12.1::q12.1::p15.5::p15.4::p11.2::q12.1::) chr11:g[47963807_cen_57123447inv::34232223_34232228::34232469_34232519::CACAGCTATGAGA::57123447_chr11:57150478::TTTCCATTCCA::chr11:1791532_chr11:1831828::chr11:3681909_chr11:3826675::AGAGATGGAGCAAGCAATAGCAACTGCATA::chr11:45940475_45998725::CACTGTAAATTGGG::47277430_47429775inv::chr11:57151476_57152981inv] chr11:g[57452438_57453327::57150508_57151481inv::5745145_57452437::57276408_5728946::18428101_18558839::57278947_57297284inv]
	sSMC11_11b	chr11:3681909-3826675	p15.4	144 kb	Dup	BPJ_11g(+)_11a(+): 11bp nontemplated insertion	
	sSMC11_11c	chr11:18428101-18558839	p15.1	130 kb	Dup	BPJ_11a(+)_11b(+): blunt fusion	
	sSMC11_11d	chr11:45940475-45998725	p11.2	58kb	Dup	BPJ_11b(+)_11d(+): 30bp non-templated insertion	
	sSMC11_11e	Chr11:47277430-47429775	p11.2	152 kb	Dup	BPJ_11d(+)_11e(-): 14bp non-templated insertion	
	sSMC11_11f	chr11:47963807-57123447	p11.2.q12.1	9,1 Mb	Dup	BPJ_11l(+)_11h1(-): 8bp microhomology	
	sSMC11_11g	Chr11:57123448-57150478	q12.1	27kb	Dup	BPJ_11k(+)_11i(+): 3bp microhomology	
	sSMC11_11h1	Chr11:57150508-57151481	q12.1	967 bp	Dup	BPJ_11c(+)_11j(-): blunt fusion	
	sSMC11_11h2	Chr11:57151476-57152981	q12.1	1,5kb	Dup		

	sSMC11_11i1	Chr11: 57152982-57276407	q12.1	123 kb	Dup		
	sSMC11_11i2	Chr11:57276408-57278946	q12.1	2,5kb	Dup		
	sSMC11_11j	Chr11:57278947-57297284	q12.1	18,3 kb	Dup		
	sSMC11_11k	Chr11:57451445-57452437	q12.1	992 bp	Dup		
	sSMC11_11l	Chr11:57452438-57453327	q12.1	896 bp	Dup		
sSMC17	sSMC17_17b	chr17:16,958,801-19,954,445	17p11.2	2,9 Mb	Dup	BPJ_17d(+)_17b(+):36bp insertion (LINE-1)	seq[GRCh37] +der(17)(q11.2::p11.2->q11.2::p11.2) chr17:g.[26893603_28644215::22251490~_cen_26140775::AAGGGTTAATTCTTTTATATGTTGTATTTTAGTAG::16958801_19954445]add
	sSMC17_17d	chr17:21,700,105-26,140,775	17p11.2.q11.2	4,4 Mb	Dup		
	sSMC17_17f	chr17:26,893,603-28,644,215	17q11.2	1,6 Mb	Dup		

Supplementary figures and tables

sSMC18	sSMC18_18b	chr18:18,520,343-18,594,804	18q11.1	74,4 kb	Dup	BPJ_18b(+)_18d(+): microhomology of 4bp(ATGG), RingJ_18d(+)_Alphoid: microhomology of 4bp(GAGC)	seq[GRCh37] +r(18) (:q11.1::q12.3->q21.2::) chr18:g.[cen_18520343_18594804::41472065_49040431::Alphoid DNA L1.84]add
	sSMC18_18d	chr18:41472065-49040431	18q12.3.q21.2	7,5 Mb	Dup		

## References

**Ahram DF, Stambouli D, Syrogianni A, Al-Sarraj Y, Gerou S, El-Shanti H and Kambouris M.** Mosaic partial pericentromeric trisomy 8 and maternal uniparental disomy in a male patient with autism spectrum disorder. *Clin. Case Reports.* 2016;4(12):1125–31

**Bertelsen B, Nazaryan-Petersen L, Sun W, Mehrjouy MM, Xie G, Chen W, Hjerminde LE, Taschner PEM and Tümer Z.** A germline chromothripsis event stably segregating in 11 individuals through three generations. *Genet. Med.* 2015;18(4):494–500.

**Blyth M, Maloney V, Beal S, Collinson M, Huang S, Crolla J, Temple I. K, and Baralle D.** Pallister-killian syndrome: a study of 22 british patients. *J. Med. Genet.* 2015;52(7):454–64.

**Callen DF, Freemantle CJ, Ringenbergs ML, Baker E, Eyre HJ, Romain D and Haan E.** The isochromosome 18p syndrome: confirmation of cytogenetic diagnosis in nine cases by in situ hybridization. *Am. J. Hum. Genet.* 1990;47(3):493–98.

**Chantot-Bastarud S, Stratmann S, Brioude F, Begemann M, Elbracht M, Graul-Neumann L, Harbison M, Netchine I and Eggermann, T.** Formation of upd(7)mat by trisomic rescue: snp array typing provides new insights in chromosomal nondisjunction. *Mol. Cytogenet.* 2017;10(1):1–7.

**Chen X, Schulz-Trieglaff O, Shaw R, Barnes B, Schlesinger F, Källberg M, Cox AJ, Kruglyak S and Saunders CT.** Manta: rapid detection of structural variants and indels for germline and cancer sequencing applications. *Bioinformatics.* 2016;32(8):1220–22.

**Chiang C, Jacobsen JC, Ernst C, Hanscom C, Heilbut A, Blumenthal I, Mills RE, Kirby A, Lindgren AM, Rudiger SR, McLaughlan CJ, Bawden CS, Reid SJ, Faull RLM, Snell RG et al.** Complex reorganization and predominant non-homologous repair following chromosomal breakage in karyotypically balanced germline rearrangements and transgenic integration. *Nat. Genet.* 2012;44(4):390–397.

**Conlin LK, Kaur M, Izumi K, Campbell L, Wilkens A, Clark D, Deardorff MA, Zackai EH, Pallister P, Hakonarson H, Spinner NB and Krantz ID.** Utility of SNP arrays in detecting, quantifying, and determining meiotic origin of tetrasomy 12p in blood from individuals with Pallister-Killian syndrome. *Am. J. Med. Genet.* 2012;158(12):3046–3053.

**Crasta K, Ganem, NJ, Dagher R, Lantermann AB, Ivanova EV, Pan Y, Nezi L, Protopopov A, Chowdhury D and Pellman D.** DNA breaks and chromosome pulverization from errors in mitosis. *Nature*. 2012;482(7383):53–58

**Crolla JA, Harvey JF, Sitch FL and Dennis NR.** Supernumerary marker 15 chromosomes: a clinical, molecular and FISH approach to diagnosis and prognosis. *Hum. Genet.* 1995;95(2): 161–170.

**Crolla JA, Youngs SA, Ennis S and Jacobs PA.** Supernumerary marker chromosomes in man: parental origin, mosaicism and maternal age revisited. *Eur. J. Hum. Genet.* 2005;13(2):154–160.

**Franasiak JM, Forman EJ, Hong KH, Werner MD, Upham KM, Treff NR and Scott RTJ.** The nature of aneuploidy with increasing age of the female partner: a review of 15,169 consecutive trophoctoderm biopsies evaluated with comprehensive chromosomal screening. *Fertil. and Steril.* 2014;101(3):656–663.

**Graf MD, Christ L, Mascarello JT, Mowrey P, Pettenati M, Stetten G, Storto P, Surti U, Van Dyke DL, Vance GH, Wolff D and Schwartz S.** Redefining the risks of prenatally ascertained supernumerary marker chromosomes: a collaborative study. *J. Med. Genet.* 2006;43(8):660–4.

**Hahnemann JM and Vejerslev LO.** European collaborative research on mosaicism in CVS (EUCROMIC)--fetal and extrafetal cell lineages in 192 gestations with CVS mosaicism involving single autosomal trisomy. *Am. J. Med. Genet.* 1997;70(2):179–187.

**Hartwig TS, Ambye L, Sorensen S and Jorgensen FS.** Discordant non-invasive prenatal testing (NIPT) - a systematic review. *Prenat. Diagn.* 2017;37(6):527–539.

**Hastings PJ, Ira G and Lupski JR.** A Microhomology-Mediated Break-Induced Replication Model for the Origin of Human Copy Number Variation. *PLOS Genet.* 2009;5(1):1–9.

**Hatch EM.** Catastrophic nuclear envelope collapse in cancer cell micronuclei. *Cell.* 2013;154(1):47–60.

**Hoffelder D, Luo L, Burke N, Watkins S, Gollin S and Saunders W.** Resolution of anaphase bridges in cancer cells. *Chromosoma.* 2004;112(8):389–397.

**Janssen A, van der Burg M, Szuhai K, Kops GJPL and Medema RH.** Chromosome segregation errors as a cause of DNA damage and structural chromosome aberrations. *Science.* 2011; 333(6051):1895–1898.

**Kalousek DK and Dill FJ.** Chromosomal mosaicism confined to the placenta in human conceptions. *Science*. 1983;221(4611):665–7.

**Kalousek DK and Vekemans M.** Confined placental mosaicism. *J. Med. Genet.* 1996;33(7):529–533.

**Kato T, Ouchi Y, Inagaki H, Makita Y, Mizuno S, Kajita M, Ikeda T, Takeuchi K and Kurahashi H.** Genomic Characterization of Chromosomal Insertions: Insights into the Mechanisms Underlying Chromothripsis. *Cytogenet. and Genome Res.* 2017;1192:1–9.

**King DA, Fitzgerald TW, Miller R, Canham N, Clayton-Smith J, Johnson D, Mansour S, Stewart F, Vasudevan P and Hurles ME.** A novel method for detecting uniparental disomy from trio genotypes identifies a significant excess in children with developmental disorders. *Genome Res.* 2014;24(4):673–687.

**Klein E, Rocchi M, Ovens-Raeder A, Kosyakova N, Weise A, Ziegler M, Meins M, Morlot S, Fischer W, Volleth M, Polityko A, Ogilvie CM, Kraus C and Liehr T.** Five novel locations of Neocentromeres in human: 18q22.1, Xq27.1 approximately 27.2, Acro p13, Acro p12, and heterochromatin of unknown origin. *Cytogenet. and Genome Res.* 2012;136(3):163–166.

**Kloosterman WP, Guryev V, van Roosmalen M, Duran KJ, de Bruijn E, Bakker SCM, Letteboer T, van Nesselrooij B, Hochstenbach R, Poot M, Cuppen E.** Chromothripsis as a mechanism driving complex de novo structural rearrangements in the germline. *Hum. Mol. Genet.* 2011;20(10):1916–1924.

**Kloosterman, W. P., Tavakoli-Yaraki, M., Van Roosmalen, M. J., Van Binsbergen, E., Renkens, I., Duran, K., Ballarati L, Vergult S, Giardino D, Hansson K, Ruivenkamp CAL, Jager M, van Haeringen A, Ippel EF, Haaf T et al.** Constitutional Chromothripsis Rearrangements Involve Clustered Double-Stranded DNA Breaks and Nonhomologous Repair Mechanisms. *Cell Rep.* 2012;1(6):648–655.

**Kotzot D.** Supernumerary marker chromosomes (SMC) and uniparental disomy (UPD): coincidence or consequence? *J. Med. Genet.* 2002;39:775–778.

**Layer RM, Chiang C, Quinlan AR and Hall IM.** LUMPY: a probabilistic framework for structural variant discovery. *Genome Biol.* 2014;15(6)

**Lee JA, Carvalho CMB, and Lupski JR.** A DNA replication mechanism for generating nonrecurrent rearrangements associated with genomic disorders. *Cell*. 2007;131(7):1235–1247.

**Liang J, Cai W and Sun Z.** Single-cell sequencing technologies: current and future. *J. Genet. Genomics*. 2014; 41(10):513–528.

**Liehr T, Claussen U and Starke H.** Small supernumerary marker chromosomes (sSMC) in humans. *Cytogenet. Genome Res*. 2004;107:55–67.

**Liehr T, Ewers E, Hamid AB, Kosyakova N, Voigt M, Weise A and Manvelyan M.** Small Supernumerary Marker Chromosomes and Uniparental Disomy Have a Story to Tell. *J. Histochem. Cytochem*. 2015;59(9):842–848.

**Liehr T and Weise A.** Frequency of small supernumerary marker chromosomes in prenatal, newborn, developmentally retarded and infertility diagnostics. *Int. J. Mol. Med*. 2007;19(5):719–731.

**Liu P, Erez A, Nagamani SCS, Dhar SU, Kołodziejska KE, Dharmadhikari AV, Cooper ML, Wiszniewska J, Zhang F, Withers MA, Bacino CA, Campos-Acevedo LD, Delgado MR, Freedenberg D, Garnica A et al.** Chromosome catastrophes involve replication mechanisms generating complex genomic rearrangements. *Cell*. 2011;146(6):889–903.

**Lupski JR and Stankiewicz P.** Genomic Disorders: Molecular Mechanisms for Rearrangements and Conveyed Phenotypes. *PLOS Genet*. 2005;1(6):1–7.

**Ly P and Cleveland DW.** Interrogating cell division errors using random and chromosome-specific missegregation approaches. *Cell Cycle*. 2017;16(13):1252–1258.

**Ly P, Teitz LS, Kim DH, Shoshani O, Skaletsky H, Fachinetti D, Page DC and Cleveland DW.** Selective Y centromere inactivation triggers chromosome shattering in micronuclei and repair by non-homologous end joining. *Nat. Cell Biol*. 2017;19(1):68–75

**Malhotra A, Lindberg M, Faust GG, Leibowitz ML, Clark RA, Layer RM, Quinlan AR and Hall IM.** Breakpoint profiling of 64 cancer genomes reveals numerous complex rearrangements spawned by homology-independent mechanisms. *Genome Res*. 2013;23(5):762–776.

**Malvestiti F, De Toffol S, Grimi B, Chinetti S, Marcato L, Agrati C, Di Meco AM, Frascoli G, Trotta A, Malvestiti B, Ruggeri A, Dulcetti F, Maggi F, Simoni G, Grati FR and Grati FR.** De novo small supernumerary marker chromosomes detected on 143000 consecutive

prenatal diagnoses: Chromosomal distribution, frequencies, and characterization combining molecular cytogenetics approaches. *Prenat. Diagn.* 2014;34(5):460–468.

**Marle N, Martinet D, Aboura A, Joly-Helas G, Andrieux J, Flori E, Puechberty J, Vialard F, Sanlaville D, Fert Ferrer S, Bourrouillou G, Tabet AC, Quilichini B, Simon-Bouy B, Bazin A et al.** Molecular characterization of 39 de novo sSMC: contribution to prognosis and genetic counselling, a prospective study. *Clin. Genet.* 2014;85(3):233–244.

**Mears AJ.** Minute Supernumerary Ring Chromosome 22 Associated with Cat Eye Syndrome: Further Delineation. *Am. J. Hum. Genet.* 1995;57:667-673.

**Melo BCS, Portocarrero A, Alves C, Sampaio A and Mota-Vieira L.** Paternal Transmission of Small Supernumerary Marker Chromosome 15 Identified in Prenatal Diagnosis Due to Advanced Maternal Age. *Clin. Med. Insights. Case Rep.* 2015;8, 93–96.

**Murmann AE, Conrad DF, Mashek H, Curtis CA, Nicolae RI, Ober C and Schwartz S.** Inverted duplications on acentric markers: mechanism of formation. *Hum. Mol. Genet.* 2009;18(12):2241–56.

**Nagaoka SI, Hassold TJ and Hunt PA.** Human aneuploidy: Mechanisms and new insights into an age-old problem. *Nat. Rev. Genet.* 2012;13(7):493–504

**Nazaryan-Petersen L, Bertelsen B, Bak M, Jønson L, Tommerup N, Hancks DC and Tümer, Z.** Germline Chromothripsis Driven by L1-Mediated Retrotransposition and Alu/Alu Homologous Recombination. *Hum. Mutat.* 2016;37(4):385–395.

**Nicholson JM, Macedo JC, Mattingly AJ, Wangsa D, Camps J, Lima V, Gomes AM and Cimini D.** Chromosome mis-segregation and cytokinesis failure in trisomic human cells. *Elife.* 2015;4:1–23.

**Obe G, Lüdcke JBP, Waldenmaier K and Sperling K.** Premature chromosome condensation in a case of Fanconi's anemia. *Hum. Genet.* 1975;28(2):159–162.

**Raczy C, Petrovski R, Saunders CT, Chorny I, Kruglyak S, Margulies EH, Chuang HY, Kallberg M, Kumar SA, Liao A, Little KM, Strömberg MP and Tanner SW.** Isaac: Ultra-fast whole-genome secondary analysis on Illumina sequencing platforms. *Bioinformatics.* 2013;29(16):2041–2043.

**Robinson JT, Thorvaldsdóttir H, Winckler W, Guttman M, Lander ES, Getz G and Mesirov JP.** Integrative Genome Viewer. *Nat. Biotechnol.* 2011;29(1):24–6.

**Robinson WP.** Mechanisms leading to uniparental disomy and their clinical consequences. *BioEssays.* 2000;22(5):452–459.

**Rothlisberger B.** A supernumerary marker chromosome originating from two different regions of chromosome 18. *J. Med. Genet.* 2000;37:121–124.

**Schinzel A.** Tetrasomy 12p (Pallister-Killian syndrome). *J. Med. Genet.* 1991;28(2):122–5.

**Schreck RR, Breg WR, Erlanger B and Miller OJ.** Preferential derivation of abnormal human G-group-like chromosomes from chromosome 15. *Hum. Genet.* 1977;36:1–12.

**Sen S, Hittelman WN, Teeter LD and Kuo MT.** Model for the Formation of Double Minutes from Prematurely Condensed Chromosomes of Replicating Micronuclei in Drug-treated Chinese Hamster Ovary Cells Undergoing DNA Amplification. *Cancer Res.* 1989;49(23):6731–6737.

**Shaikh TH, Budarf ML, Celle L, Zacka EH and Emanuel BS.** Clustered 11q23 and 22q11 breakpoints and 3:1 meiotic malsegregation in multiple unrelated t(11;22) families. *Am. J. Hum. Genet.* 1999;65(6):1595–607.

**Sheth F, Ewers E, Kosyakova N, Weise A, Sheth J, Patil S, Ziegler M and Liehr T.** A neocentric isochromosome Yp present as additional small supernumerary marker chromosome--evidence against U-type exchange mechanism? *Cytogenet. Genome Res.* 2009;125:115–116.

**Spielmann M, Lupiáñez DG and Mundlos S.** Structural variation in the 3D genome. *Nat. Rev. Genet.* 2018;19(7):453–467.

**Srebniak M, Boter M, Oudesluijs G, Joosten M, Govaerts L, Van Opstal D and Galjaard, R. J. H.** Application of SNP array for rapid prenatal diagnosis: implementation, genetic counselling and diagnostic flow. *Eur. J. Hum. Genet.* 2011;19(12):1230–1237.

**Stephens PJ, Greenman CD, Fu B, Yang F, Bignell GR, Mudie LJ, Pleasance ED, Lau KW, Beare D, Stebbings LA, McLaren S, Meng-Lay L, McBride DJ, Varela I, Nik-Zainal S et al.** Massive Genomic Rearrangement Acquired in a Single Catastrophic Event during Cancer Development. *Cell.* 2011;144:27–40.

**Terradas M, Martín M, Tusell L and Genescà A.** DNA lesions sequestered in micronuclei induce a local defective-damage response. *DNA Repair*. 2009;8(10):1225–1234.

**Terradas M, Martín M, Tusell L and Genescà A.** Genetic activities in micronuclei: Is the DNA entrapped in micronuclei lost for the cell? *Mutat. Res*. 2010;705(1):60–67.

**Trinkaus E.** Late Pleistocene adult mortality patterns and modern human establishment. *Proc. Natl. Acad. Sci. U. S. A.* 2011;108(4):1267–1271.

**Vetro A, Manolakos E, Petersen MB, Thomaidis L, Liehr T, Croci G, Franchi F, Marinelli, M, Meneghelli E, Dal Bello B, Cesari S, Iasci Angela, Arrigo G and Zuffardi O.** Unexpected results in the constitution of small supernumerary marker chromosomes. *Eur. J. Med. Genet*. 2012;55(3):185–190.

**Vialard F, Molina-Gomes D, Quarello E, Leroy B, Ville Y and Selva J.** Partial chromosome deletion: a new trisomy rescue mechanism? *Fetal Diagn. Ther.* 2009;25(1):111–114.

**Voullaire L, Saffery R, Earle E, Irvine DV, Slater H, Dale S, Du Sart D, Fleming T and Choo KHA.** Mosaic Inv Dup(8p) Marker Chromosome With Stable Neocentromere Suggests Neocentromerization Is a Post-Zygotic Event. *Am. J. Med. Genet*. 2001;102:86–94.

**Wang S, Hassold T, Hunt P, White MA, Zickler D, Kleckner N and Zhang L.** Inefficient crossover maturation underlies elevated aneuploidy in human female meiosis. *Cell*. 2017;168 (6):977–989.e17.

**Warburton D.** Reproductive loss: how much is preventable? *N. Engl. J. Med.* 1987.

**Zhang C-Z, Spektor A, Cornils H, Francis JM, Jackson EK, Liu S, Meyerson M and Pellman D.** Chromothripsis from DNA damage in micronuclei. *Nature*. 2015;522(6):179–184.

## **List of original manuscripts**

**Kurtas NE**, Xumerle L, Leonardelli L, Delledonne M, Brusco A, Chrzaowska K, Schinzel A, Larizza D, Gueneri S, Natacci F, Bonaglia MC, Reho P, Manolakos E, Mattina T, Soli F, Provenzano A, Al-Rikabi AH, Errichiello E, Nazaryan-Petersen L, Giglio S, Tommerup N, Liehr T and Zuffardi O. Small supernumerary marker chromosomes: a legacy of trisomy rescue?. 2018 (SUBMITTED).

Bonaglia MC, **Kurtas NE**, Errichiello E, Bertuzzo S, Beri S, Mehrjouy MM, Provenzano A, Vergani D, Pecile V, Novara F, Reho P, Di Giacomo MC, Discepoli G, Giorda R, Aldred MA, Santos-Rebouças CB, Goncalves AP, Abuelo DN, Giglio S, Ricca I, Franchi F, Patsalis P, Sismani C, Morí MA, Nevado J, Tommerup N and Zuffardi O. de novo unbalanced translocations have a complex history/aetiology. *Hum. Genet.* 2018 (IN PRESS).

**Kurtas NE**, Xumerle L, Giussani U, Pansa A, Cardarelli A, Bertini<sup>5</sup>, Angelo Valetto V, Liehr T, Bonaglia MC, Errichiello E, Delledonne M and Zuffardi O. Insertional translocation in three cases of constitutional chromothripsis involving an additional non-chromothriptic chromosome. *Mol. Genet. Genomic Med.* 2018 (IN PRESS).

**Kurtas N**, Arrigoni F, Errichiello E, Zucca C, Maghini C, D'Angelo MG, Beri S, Giorda R, Bertuzzo S, Delledonne M, Xumerle L, Rossato M, Zuffardi O, Bonaglia MC. Chromothripsis and ring chromosome 22: a paradigm of genomic complexity in the Phelan-McDermid syndrome (22q13 deletion syndrome). *J. Med. Genet.* 2018;55(4):269–277.

Errichiello E, Gorgone C, Giuliano L, Iadarola B, Cosentino E, Rossato M, **Kurtas NE**, Delledonne M, Mattina T, Zuffardi O. SOX2: Not always eye malformations. Severe genital but no major ocular anomalies in a female patient with the recurrent c.70del20 variant. *Eur. J. Med. Genet.* 2018;61(6):335-340.